

## **Distribution Agreement**

In presenting this thesis or dissertation as a partial fulfillment of the requirements for an advanced degree from Emory University, I hereby grant to Emory University and its agents the non-exclusive license to archive, make accessible, and display my thesis or dissertation in whole or in part in all forms of media, now or hereafter known, including display on the world wide web. I understand that I may select some access restrictions as part of the online submission of this thesis or dissertation. I retain all ownership rights to the copyright of the thesis or dissertation. I also retain the right to use in future works (such as articles or books) all or part of this thesis or dissertation.

Signature:

---

Kevin P. Hannon

---

Date

Efficient implementations of quantum chemistry methods for strongly  
correlated electrons

By

Kevin P. Hannon  
Masters of Science  
Chemistry

---

Dr. Francesco A. Evangelista, Ph.D  
Advisor

---

Dr. Joel M. Bowman, Ph.D  
Committee Member

---

Dr. Michael C. Heaven, Ph.D  
Committee Member

Accepted:

---

Lisa A. Tedesco, Ph.D  
Dean of the James T. Laney School of Graduate Studies

---

Date

Efficient implementations of quantum chemistry methods for strongly  
correlated electrons

By

Kevin P. Hannon  
B.S., Virginia Tech, 2014

Advisor: Dr. Francesco A. Evangelista, Ph.D

An abstract of  
A thesis submitted to the Faculty of the  
James T. Laney School of Graduate Studies of Emory University  
in partial fulfillment of the requirements for the degree of  
Masters of Science  
in Chemistry  
2017

## Abstract

### Efficient implementations of quantum chemistry methods for strongly correlated electrons

By Kevin P. Hannon

Strong correlation presents a big challenge in modern day quantum chemistry. In many chemical systems such as open-shell species, excited states, and transition metal complexes, one electron configuration is not flexible enough to describe these systems. This thesis is concerned with two topics: developing a parallel algorithm for a zeroth order description of strong correlation and developing a fast multireference perturbation theory for achieving quantitative accuracy. We aim to develop theories that are computationally efficient, widely applicable to various areas of chemistry, and achieve quantitative accuracy. In chapter II, we report an implementation of the atomic orbital complete active space self consistent field (AO-CASSCF) method on a massively parallel computer using a combination of distributed and multicore computing. We demonstrate the scalability of the AO-CASSCF algorithm with a benchmark set of systems. In chapter III, we report an efficient implementation of a second-order multireference perturbation theory based on the driven similarity renormalization group (DSRG-MRPT2) [C. Li and F. A. Evangelista, *J. Chem. Theory Comput.* **11**, 2097 (2015)]. Our implementation employs factorized two-electron integrals to avoid storage of large four-index intermediates. It also exploits the block structure of the reference density matrices to reduce the computational cost to that of second-order Møller–Plesset perturbation theory. Our new DSRG-MRPT2 implementation is benchmarked on ten naphthylene isomers using basis sets up to quintuple- $\zeta$  quality. We find that the singlet-triplet splittings ( $\Delta_{ST}$ ) of the naphthylene isomers strongly depend on the equilibrium structures. For a consistent set of geometries, the  $\Delta_{ST}$  values predicted by the DSRG-MRPT2 are in good agreements with those computed by the reduced multireference coupled cluster theory with singles, doubles, and perturbative triples.

Efficient implementations of quantum chemistry methods for strongly  
correlated electrons

By

Kevin P. Hannon  
B.S., Virginia Tech, 2014

Advisor: Dr. Francesco A. Evangelista, Ph.D

A thesis submitted to the Faculty of the  
James T. Laney School of Graduate Studies of Emory University  
in partial fulfillment of the requirements for the degree of  
Masters of Science  
in Chemistry  
2017

## Acknowledgement

There are many people that I should thank for this thesis, but the main one is my Legal Guardian, Dr. Dean Donald Fetterolf. From a young age, he influenced my career path and taught me the beauty of science. I remember being impressed by his wisdom and knowledge. I would like to thank him for all the wisdom he has imparted on me throughout the years.

I would also like to thank my Advisor, Dr. Evangelista and my group members for providing excellent feedback throughout my short graduate career. Jeffrey Schriber, Prakash Verma, Tianyan Zhang, Chenyang (York) Li, and Wallace Derricotte provided excellent advice during my tenure as a graduate student. I am happy that I met these 5 during my time.

# Table of Contents

<b>1</b>	<b>Introduction</b>	<b>1</b>
1.1	Introduction	1
1.1.1	Static correlation	1
1.1.2	Dynamic Correlation	4
1.2	Layout of the thesis	5
<b>2</b>	<b>A MPI/OpenMP implementation of Atomic-Orbital Complete Active Space Self Consistent Field Method</b>	<b>6</b>
2.1	Introduction	6
2.2	AO-CASSCF	8
2.3	Results	10
2.3.1	Ethylene and Water	11
2.3.2	Spin splittings in TM complexes	13
2.3.3	Polycarbene	15
2.4	Conclusion	16
2.5	Acknowledgments	17
2.6	Appendix	17
<b>3</b>	<b>An integral-factorized implementation of the driven similarity renormalization group second-order multireference perturbation theory</b>	<b>20</b>
3.1	Introduction	20
3.2	Theory	24
3.2.1	The MR-DSRG formalism	24
3.2.2	The DSRG-MRPT2 method	25
3.2.3	Integral factorizations	28
3.3	Implementation	29
3.4	Computational Details	34
3.5	Results	36
3.5.1	Singlet-triplet splittings of naphthyne diradicals	36
3.5.2	Scaling with respect to basis set and active space size	42
3.6	Conclusion	44

# List of Figures

1.1	A basic description of the difference between static (nondynamical) correlation and dynamic correlation. Static correlation is the correlation gained via CASSCF and dynamic correlation is typically gained through more approximate means. This figure is reprinted with permission from Ref 14. . . . .	3
2.1	Ethylene solvated by 115 waters. The structures were generated using TIP3P waters with a solvation shell of 1.5 Å . . . . .	12
2.2	Ethylene solvated by 115 waters. Speed-ups are done relative to 64 cores. We show the speed-ups for the integral transformation, the orbital gradient, and the overall timings for AO-CASSCF. . . . .	12
2.3	A large transition metal complex used as a test set for computing spin splittings. The molecule is a Copper oxalate compound. . . . .	14
2.4	Speed-ups for the integral transformation, orbital gradient, and the overall iteration for CuOC. A def2-SVP basis set with 970 basis functions was used. All speed-ups were done relative to 8 cores. The value on the graph represents the overall time for 1024 cores. . . . .	14
2.5	Speed-ups for the integral transformation, orbital gradient, and the overall iteration for CuOC. A def2-TZVP basis set with 1726 basis functions was used. All speed-ups were computed relative to 16 cores. The value on the graph represents the overall time for 2048 cores. . . . .	14
3.1	The structures of one-particle density matrix $\gamma_q^p$ and one-hole density matrix $\eta_q^p$ . Non-zero elements of the one-particle and one-hole density matrices are indicated respectively in red and blue. . . . .	30
3.2	The scaling of diagram F1 of Table 3.2 for (2,3)-naphthylene using a cc-pVTZ basis set. The speed up is determined as $\frac{S(1)}{S(N)}$ where $S(i)$ is the total time required to evaluate this term using $i$ threads. Results are for up to 8 threads on an Intel Xeon E5-2650 v2 processor. . . . .	32

3.3	This figure illustrates the ability of the AMBIT tensor library to deal with block-sparse tensors that span composite orbital space. The tensor contraction shown at the top involves a summation over the index $j$ that spans the generalized orbitals space ( <b>H</b> ), which is the union of the core ( <b>C</b> ) and active ( <b>A</b> ) orbitals. The tensors $\gamma_i^j$ and $t_a^i$ are defined over subsets (shown in orange) of the full orbital indices and are block sparse. For example, the <b>A-A</b> block of $t_a^i$ is zero because internal amplitudes are not defined in the DSRG-MRPT2. AMBIT allows to write contractions over block-sparse tensors as contractions over composite index tensors, thus, reducing the number of equations required to include in the source code. . . . .	33
3.4	Naphthalene numbering scheme used in this study. The notation $(i, j)$ -naphthyne indicates that two hydrogen atoms were removed from positions $i$ and $j$ . . . . .	34
3.5	Example of a transition metal complex, $[(\text{Et}_5\text{dien})_2\text{Cu}_2^{\text{II}}(\mu\text{-C}_2\text{O}_4)]^{2+}$ , that can be treated with the DF-DSRG-MRPT2 approach. Singlet state computed with a CAS(2,2) active space, ROHF triplet orbitals, and the def2-TZVP basis set (1726 basis functions). The DF-DSRG-MRPT2 computation ran in about 5.2 hours on a Intel Xeon E5-2650 v2 processor using 8 threads. Geometry taken from Ref. 186. . . . .	43

# List of Tables

2.1	Speed-ups, efficiencies, and overall for CASSCF computation . . . . .	11
2.2	Speed-ups, efficiencies, and overall for CASSCF computation with both the def2-SVP and def2-TZVP basis sets. Overall timing corresponds to the the entire CASSCF procedure. Speed-up is defined as $\frac{S(N)}{S(8)}$ for def2-SVP and $\frac{S(N)}{S(16)}$ for def2-TZVP. . . . .	15
2.3	The performance of the DG algorithm for polycarbene with a density group of 1, 5, and 11, respectively. The timings are for one integral transformation. . . . .	16
3.1	DSRG-MRPT2 energy contributions. Following the Einstein convention, summation over repeated indices is assumed. Asymptotic cost scalings are given in big $\mathcal{O}$ notation. . . . .	28
3.2	DSRG-MRPT2 energy terms that arise from diagram F after taking into account the block structure of the one-hole and one-particle density matrices. Contractions involving the one-particle density matrix ( $\gamma_j^i$ ) and hole indices are indicated with a red circle, while contractions of the one-hole density matrix ( $\eta_b^a$ ) and particle indices are indicated with a blue circle. . . . .	31
3.3	Point group symmetries for all naphthyne isomers along with the corresponding minimal active spaces in Cotton’s ordering.[169] We use the following ordering for $C_s$ , $C_{2v}$ and $C_{2h}$ : $(a', a'')$ , $(a_1, a_2, b_1, b_2)$ , and $(a_g, b_g, a_u, b_u)$ . For example, the notation (2, 10) means that the active space is composed of two $a'$ orbitals and ten $a''$ orbitals. For (1,4)-, (1,8)-, (2,3)-, and (2,7)-naphthyne, the molecules are placed in the $xz$ plane, where $z$ is the $C_2$ rotation axis. All other naphthyne are placed in the $xy$ plane. . . . .	35
3.4	Analysis of the DSRG-MRPT2 energy error (in kcal mol <sup>-1</sup> ) introduced by density fitting (DF) and Cholesky decomposition (CD). Statistics were computed from the singlet-triplet splittings of the ten naphthyne isomers. Density fitting results were obtained using the cc-pVDZ-RI auxiliary basis set, while Cholesky vectors were generated using a threshold of $10^{-5} E_h$ . . . . .	36
3.5	Adiabatic singlet-triplet splittings ( $\Delta E_{ST} = E_S - E_T$ ) of naphthyne diradicals computed with the DF-DSRG-MRPT2 approach and a variety of basis sets. All computations utilized ROHF triplet orbitals. Carbon 1s-like orbitals were excluded from the DSRG-MRPT2 treatment of correlation energy. . . . .	37

3.6	Adiabatic singlet-triplet splittings ( $\Delta E_{\text{ST}} = E_{\text{S}} - E_{\text{T}}$ ) of naphthyne diradicals computed with the DSRG-MRPT2, CASPT2, and RMR-CCSD(T) approaches. All DSRG-MRPT2 computations used triplet ROHF orbitals and the cc-pVDZ-RI auxiliary basis set. RMR-CCSD(T) results used RHF and ROHF orbitals for singlet and triplet states, respectively. CASPT2 results used CASSCF(12,12) orbitals. RMR-CCSD(T) and DSRG-MRPT2 results are based on the same geometries (from DFT and CASSCF, see Sec. 3.4), while CASPT2 results are based on CASSCF(12,12) optimized geometries. The VDZ* basis set is constructed from the cc-pVDZ basis set by removing hydrogen $p$ functions. . . . .	39
3.7	A comparison of the vertical singlet-triplet splitting between MRCC and the DSRG-MRPT2. All of these results use singlet geometries, RHF orbitals, and a CAS(2,2). . . . .	41
3.8	Timing of DSRG-MRPT2 naphthyne computations ( $T_{\text{PT2}}$ , in seconds) as a function of basis set size ( $N$ ). The total time ( $T$ ) includes the CASCI step, generation of the DF integrals, and evaluation of the DSRG-MRPT2 energy. These computations ran on one Intel Xeon E5-2650 v2 processor using 8 threads. . . . .	43

# Chapter 1 Introduction

## 1.1 Introduction

In the past 20 years, density functional theory (DFT) has become the most commonly used quantum chemistry method. [1, 2] Among the factors that have contributed to the success of DFT, the most important ones are: (i) a good balance between cost and accuracy and (ii) the fact that DFT is a black-box approach that requires little input from the user. However, DFT can perform poorly for transition metal complexes, excited states, and bond-breaking.[1] Two major problems of DFT is the reliance on a single electron configuration and a poor description of electron correlation .[3–5] In order to extend quantum chemistry to systems that require more than one electron configuration, one needs to develop methods that are widely applicable to various areas of chemistry, able to simulate larger chemical systems, and are quantitatively accurate

In this thesis, we are concerned with developing theories that satisfy those three criteria. Widely applicable methods rely on going beyond a single electron configuration. Typically, the correlation of electrons between a selected few electron configurations is called static correlation.[6] Achieving quantitative accuracy and computational efficiency require the use of economical theories to describe dynamic correlation, that is, weak correlation effects that are complementary to static correlation. [7]

### 1.1.1 Static correlation

Strong correlation can be captured (or described) using a linear combinations of Slater determinants,

$$|\Phi\rangle = \sum_i c_i |\phi_i\rangle, \quad (1.1)$$

where  $\Phi$  is the overall wavefunction,  $\phi_i$  represent Slater determinants and  $c_i$  represents a weight of the Slater determinant.

Typically, the first step of describing strong correlation is to optimize both the orbitals ( $\phi_i$ ) and the electron configuration coefficients ( $c_i$ ). To do both tasks, quantum chemists actually use similar ideas from Hartree-Fock theory.[\[8\]](#) The basic idea of Hartree-Fock is to find a basis where the Fock matrix is either diagonal or block-diagonal. In most cases, the solution is to build and diagonalize the Fock matrix. Building the Fock matrix can be done through the use of one electron integrals ( $h_{pq}$ ) and two-electron integrals  $[(pq|rs)]$ . In Hartree-Fock theory, the Fock matrix is simply,

$$F_{pq} = h_{pq} + \sum_{rs} 2 [(pq|rs) - (pr|qs)] \quad (1.2)$$

Building the Fock matrix scales as  $\mathcal{O}(N^4)$ , where  $N$  is the number of basis functions. The  $\mathcal{O}(N^4)$  scaling becomes quite expensive for larger systems. There exists two ways to scale to larger systems: Screening of the non-zero integrals[\[9, 10\]](#) and parallel computing.[\[11, 12\]](#)

Chapter II discusses how to implement a fast algorithm for computing Fock matrices through the use of integral screening and parallel computing. Integral screening is the ability to screen out near zero integrals via the use of some estimate for the magnitude. In this work, we will use the Cauchy-Schwartz inequality  $[(pq|rs) \leq |(pq|pq)^{(1/2)}|(rs|rs)^{(1/2)}]$ . The Cauchy-Schwartz inequality provides a criterion to screen out many integrals and allows the building of the Fock matrix to scale only as  $\mathcal{O}(N^2)$ . Algorithms that can take advantage of this reduced scaling can potentially expand the reach of quantum chemistry to much larger systems.[\[9, 13\]](#) Chapter 2 provides a more extensive background of how integral screening is applied for the complete active space self consistent field theory(CASSCF).

Parallel computing is a massive field of computer science. The simplest description of a parallel computer is a set of computers that communicate with each other by passing messages. The main scientific programming tool for communicating between

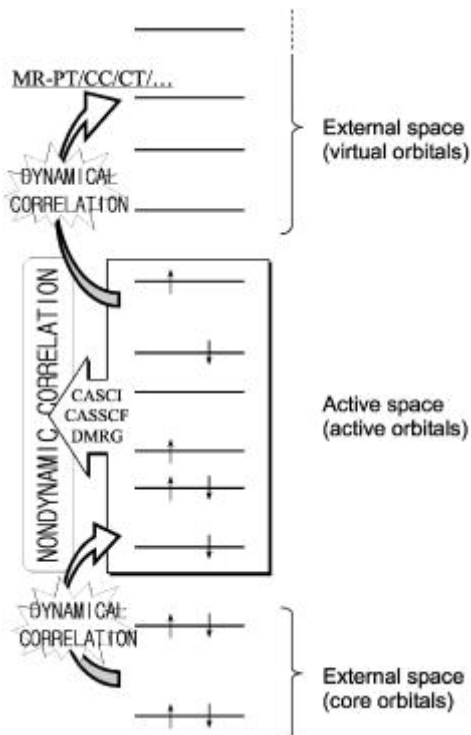


Figure 1.1: A basic description of the difference between static (nondynamical) correlation and dynamic correlation. Static correlation is the correlation gained via CASSCF and dynamic correlation is typically gained through more approximate means. This figure is reprinted with permission from Ref 14.

computers is the message passing interface (MPI).[12] Within each computer, there exists multiple threads that are capable of executing a series of instructions simultaneously. A popular library for expressing this parallelism with code is OpenMP. Chapter 2 is concerned with implementing the Fock builds with the use of both MPI and OpenMP. This means that we are using the parallelism of the different computers and the parallelism within each computer. The performance of a parallel algorithm is usually defined by Speed-up ( $\frac{S(1)}{S(N)}$ ), where  $S$  represents the overall time to solution. If you have  $N$  computers, you should have a program that is  $N$  times faster. This is an ideal speed-up, but usually the performance is measured relative to this metric. The other metric for measuring performance is parallel efficiency ( $\text{Efficiency} = \frac{S(1)}{S(N)N}$ ).

### 1.1.2 Dynamic Correlation

Both Hartree-Fock and CASSCF rely on selecting a single reference determinant or multiple determinants. CASSCF involves the distribution of electrons in orbitals and performing a matrix diagonalization. This diagonalization is expensive and can only be performed for a small subset of the total number of orbitals. Limiting the diagonalization to a subset of orbitals provides the ability to describe the relevant electron configurations (think bond-breaking, excited states, etc). However, the neglected orbitals are necessary to achieve quantitative accuracy. These orbitals are usually described via techniques such as coupled cluster theory or perturbation theory.[7] Figure 1.1 shows a basic description of a quantum chemical method. CASSCF describes the static (or nondynamical) correlation while a dynamic correlation method such as perturbation theory can describe the correlation between the active orbitals and the external orbitals.

In single reference quantum chemistry, Møller-Plesset perturbation theory of second order (MP2) is a popular technique for describing dynamic correlation. Perturbation theory needs orbital energy denominators ( $\Delta_{ijab}$ ) and two electron integrals ( $\langle ij|ab\rangle$ ),

$$E_{\text{MP2}} = \frac{1}{4} \sum_{ijab} \frac{\langle ij||ab\rangle\langle ab||ij\rangle}{\Delta_{ijab}}. \quad (1.3)$$

$$(1.4)$$

The main computational bottleneck of perturbation theory is the transformation of the integrals from the atomic orbital basis to the molecular orbital basis. This step scales as  $\mathcal{O}(N^5)$  and has  $\mathcal{O}(N^4)$  memory storage. Both of these characteristics cause MP2 to be expensive. One step that we use in this thesis to approximate the integrals

via matrix factorizations,

$$\langle ij|ab\rangle = \sum_Q B_{ia}^Q B_{jb}^Q, \quad (1.5)$$

$$B_{ia}^Q = (ia|Q). \quad (1.6)$$

$$(1.7)$$

These matrix factorizations reduce the memory storage of the two electron integrals. It is important to mention that these matrix factorizations do not reduce the overall scaling of MP2, but reduce the prefactor due to the cheaper computation of the integrals. In Chapter 3 of this thesis, we present a computationally efficient perturbation theory for describing dynamic correlation on top of a CASSCF reference. We achieve a computationally efficient method via the use of both parallelism within a node and through the use of integral factorizations.

## 1.2 Layout of the thesis

Chapter II is concerned with the development of a parallel algorithm for generating orbitals for the multireference wavefunction. We demonstrate the use of parallel algorithms for computing Fock matrices can enable CASSCF to compute much larger systems than presently done.

Chapter III is concerned with the development of an computationally efficient way of describing dynamic correlation on top of a multireference wavefunction. My contribution to this work is through the use of integral factorization techniques to greatly increase the range of systems that we can study with this multireference perturbation theory. Chapter III is published with permission from Ref. [15](#).

# Chapter 2 A MPI/OpenMP implementation of Atomic-Orbital Complete Active Space Self Consistent Field Method

## 2.1 Introduction

Computational quantum chemistry has greatly expanded the understanding of the electronic structure of closed shell molecules.[8, 16] However, there is a great interest in studying strongly correlated molecules such as transition metal present in molecular magnets[17–20] or excited states.[21–23] Many of these molecules can be quite large and it is imperative to develop new algorithms that can both simulate larger molecules and accurately describe strong correlation.

The first step of a description of strongly correlated molecules is the use of the complete active space self consistent field (CASSCF) method.[6, 24–31] CASSCF allows a description of open-shell systems and excited states by providing a zeroth-order description. However, many implementations of the CASSCF algorithm do not extend to larger systems. Recently, there has been a resurgence in applying CASSCF to larger systems via the use of integral factorizations[28, 32] or parallelization.[33–35] A major limitation of integral factorizations is that they do not reduce the overall scaling. For example, a Fock build using Cholesky decomposition[36–39] or density-fitting[40, 41] scales as  $\mathcal{O}(N^4)$ , where  $N$  is the size of the system. Without any approximations, it is very difficult to reduce the scaling to  $\mathcal{O}(N)$  or even  $\mathcal{O}(N^2)$ . [42]

Direct SCF, where direct means that the integrals are computed when needed, has played an important role in extending mean-field theories to larger molecules.[9, 13] Direct SCF avoids the asymptotic computation of all of the two electron integrals by performing screenings of the magnitude of the two electron integrals and neglecting

integrals that are below this threshold. This screening reduces the asymptotic cost of the two-electron integrals from  $\mathcal{O}(N^4)$  to  $\mathcal{O}(N^2)$ . [16]

A complementary way to extend quantum chemistry to larger molecules is to use parallelization.[12, 43] Quantum chemical implementations need some type of parallelization in order to scale both to larger systems and to reduce the time to solution. Modern supercomputer architectures take advantage of at least two levels of parallelism: message passing (MPI) and accelerators. Message passing is used to communicate among different nodes in a supercomputer system while accelerators are used to speedup the computation within a node. In recent years, there has been an increase in the use of accelerators such as Graphic Processing Units (GPUs)[44, 44–46] or the Intel Many Integrated Core Architecture.[47] A model of programming for accelerators can involve the use of both MPI and an accelerator programming language such as OpenMP or a GPU-specific language.

We intend to show that CASSCF can easily be extended to large systems via the use of MPI/OpenMP direct Fock builder. Hohenstein and coworkers recently showed the benefits of formulating a CASSCF algorithm in the atomic orbital basis while taking advantage of graphic processing units for parallelization.[33, 34] They showed that they can easily study systems up to 10000 basis functions for use in photochemistry. GPUs are of great benefit to the computational quantum chemistry community, but many of the supercomputers rely on MPI/OpenMP parallelization so it is important to have algorithms that use MPI/OpenMP parallelization. In fact, as of June 2016,[48] only two of the top 10 supercomputers use GPU architecture. In order to achieve MPI/OpenMP parallelization in the Fock builds, we adapt the Fock builder by Chow and Liu, denoted as GTFock,[49–51] for use in the algorithm developed by Hohenstein and coworkers.[33, 34]

With this new algorithm, we demonstrate the scalability of this CASSCF algorithm on two chemically relevant systems: ethylene solvated by 115 waters and an open-shell

transition metal complex. We also introduce a new algorithm that greatly reduces communication in the integral transformation when larger active spaces are used.

## 2.2 AO-CASSCF

The notation for CASSCF is presented in the supplementary information. We choose to present the major difference in this algorithm as opposed to a common CASSCF implementation. The CASSCF algorithm is summarized in Ref. 52.

The computational expensive steps of this CASSCF algorithm are the full configuration interaction (FCI) step in a limited subset of active orbitals, transforming the integrals, and forming the Fock matrices present in the orbital optimization procedure. Fletcher[35] noticed that the FCI step only starts to benefit from parallelization when there are more than ten active orbitals. For this work, we never found a case where the FCI starts to become a bottleneck. Due to this, we choose to replicate the CI on every processor. Both the integral transformation[33, 34] and the formation of the Fock matrices can be formulated in the AO basis. Formulating the Fock builds in the AO basis allows one to take advantage of the sparsity of the two electron integrals. We will denote a Fock build as  $J$  and  $K$  for a generalized Coulomb and a generalized exchange,

$$J_{\mu\nu}(D) = \sum_{\rho\sigma} (\mu\nu|\rho\sigma) D_{\rho\sigma}, \quad (2.1)$$

$$K_{\mu\nu}(D) = \sum_{\rho\sigma} (\mu\sigma|\rho\nu) D_{\rho\sigma}, \quad (2.2)$$

where  $D$  is a AO-based quantity that is to be contracted with the two electron integrals, and  $(\mu\nu|\rho\sigma)$  are the two electron integrals.

In this work, we use the parallel direct Fock builder (GTFOck) developed by Chow and coworkers.[49–51] GTFOck relies on the use of fine grained tasks to balance the computational among large number of cores while also using another scheme to assign tasks to processes to reduce communication. GTFOck relies on the Cauchy-Schwartz

screening,  $((\mu\nu|\rho\sigma) \leq (\mu\nu|\mu\nu)^{1/2}(\rho\sigma|\rho\sigma)^{1/2})$ , to avoid the computation of negligibly small integrals. GTFock is designed for heterogeneous architecture and has been demonstrated to scale to tens of thousands of cores. In this work, we choose to use the MPI/OpenMP parallelization.

The inactive Fock operator ( ${}^I F$ ) can be easily formulated as a Fock build,

$${}^I F_{pq} = \sum_{\mu\nu}^{\text{AO}} C_{\mu p} C_{\nu q} [h_{\mu\nu} + 2J_{\mu\nu}(D^{\text{core}}) - K_{\mu\nu}(D^{\text{core}})], \quad (2.3)$$

$$D_{\mu\nu}^{\text{core}} = \sum_m^{\text{Core}} C_{\mu m} C_{\nu m}, \quad (2.4)$$

$$(2.5)$$

where  $C_{\mu p}$  is the molecule orbital coefficient matrix. By back-transforming the one particle density matrix in the AO basis,

$$\gamma_{\mu\nu}^{(\text{active})} = \sum_{tu}^{\text{Active}} C_{\mu t} C_{\nu u} \gamma_{tu}, \quad (2.6)$$

$$(2.7)$$

the active Fock operator ( ${}^A F_{pq}$ ) can be formed by the Fock builder,

$${}^A F_{pq} = \sum_{\mu\nu} C_{\mu p} C_{\nu q} \left[ J_{\mu\nu}(\gamma^{(\text{active})}) - \frac{1}{2} K_{\mu\nu}(\gamma^{(\text{active})}) \right]. \quad (2.8)$$

$$(2.9)$$

The last step to formulate as a Fock build is the transformation of the integrals. Following Hohenstein and co-workers,[\[34\]](#) we form a psuedo-density for each pair  $tu$  of active orbitals,

$$P_{\mu\nu}^{(tu)} = C_{\mu t} C_{\nu u}. \quad (2.10)$$

With this psuedo-density, we can form the half transformed integrals using a Coulomb build,

$$(px|tu) = \sum_{\mu\nu}^{\text{AO}} C_{\mu p} C_{\nu x} J(P_{\mu\nu}^{(tu)}). \quad (2.11)$$

As pointed out by previous researchers,[53] without screening, this integral transformation scales as  $\mathcal{O}(N^4A^2)$ , where  $A$  is the number of active orbitals. However, the Cauchy-Schwartz screening of the integrals lowers the scaling to be between  $\mathcal{O}(A^2N)$  and  $\mathcal{O}(A^2N^2)$ . [34] A major problem with this algorithm is the strict  $\mathcal{O}(A^2)$  scaling with respect to the number of active orbitals. With the combination of post FCI methods with CASSCF, [28, 54–60] there is a resurgence in the application of CASSCF with larger active spaces than usually accessible by FCI. Extending AO-CASSCF for use with post FCI methods requires reducing the time of the integral transformation. One approach to speed-up the integral transformation is to process the number of  $A^2$  densities in parallel. We choose to use a processor subgroup algorithm where we split the MPI communicators to compute multiple densities at once and still benefit from the parallelism of GTFock. Splitting the MPI communicators lowers the amount of communication, so this allows the integral transformation to scale to more cores. Our algorithm is given below:

1. Split the processors ( $N_p$ ) into  $G$  groups.
2. Call GTFock on each  $G$  group and use  $N_G$  processors.
3. Gather the Fock matrices that were computed on each  $G$  group among the  $N_G$  processors.
4. Communicate all the Fock matrices to all the processors

## 2.3 Results

In this section, we will demonstrate the performance of our parallel CASSCF program for a transition metal complex, ethylene solvated by 115 waters, and a polycarbene complex. Tests were performed using 1 to 256 nodes (8 to 2048 cores) on the Cascade supercomputer located at the Environmental Molecular Sciences Laboratory in Pacific Northwest National Laboratory. Each node is composed of two Intel

Table 2.1: Speed-ups, efficiencies, and overall for CASSCF computation

Molecule	Cores	Overall Timing	Speed-up	Efficiency
Ethylene	64	99658	1.00	1.00
	128	49522	2.01	1.01
	256	25791	3.86	0.97
	512	14581	6.83	0.85
	1024	8749	11.39	0.71
	2048	5963	16.71	0.52

Xeon E5-2670 processors (8 cores each at 2.6 GHz) that share 128 GB of RAM. We compiled our code with icpc v 16.0.3 and linked to threaded Intel MKL. We use Intel MPI v 5.1.3. Global Arrays uses ARMCI over InfiniBand on the CASCADE machine. Our algorithm is implemented in a developer version of PSI4.[\[61\]](#)

### 2.3.1 Ethylene and Water

Another important area of CASSCF applications is the study of excited state spectra through the use of a state-averaged CASSCF and a dynamic correlation method. Since the goal of this paper is to demonstrate the scalability of the CASSCF algorithm, we choose to compute the ground state of a ethylene solvated by 115 waters. All of these computations use the cc-pVTZ basis set.[\[62\]](#) Figure [2.2](#) and Table [2.1](#) show the overall performance for ethylene with 115 waters (6787 basis functions and 351 atoms). For this larger molecule, the major limitation of the scalability of CASSCF is related to the integral transformation. The integral transformation involves transforming the integrals, computing the inactive Fock build, and various reordering procedures so we can use our FCI code. Only 60 percent of the time in the integral transformation actually involves the computing the Fock matrices. In fact, more time is spent doing the various linear algebra operations than the time spent computing the Fock matrix. By neglecting this linear algebra, our parallel performance of the Fock builds is 75 % as opposed to 55 %.

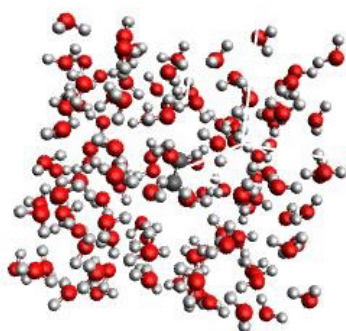


Figure 2.1: Ethylene solvated by 115 waters. The structures were generated using TIP3P waters with a solvation shell of 1.5 Å

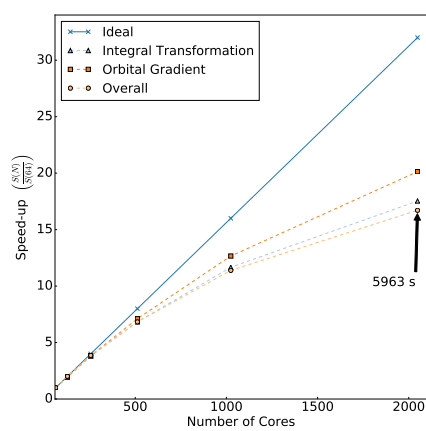


Figure 2.2: Ethylene solvated by 115 waters. Speed-ups are done to relative to 64 cores. We show the speed-ups for the integral transformation, the orbital gradient, and the overall timings for AO-CASSCF.

### 2.3.2 Spin splittings in TM complexes

Spin splittings provide an interesting challenge for CASSCF. Unlike many other methods, CASSCF provides a flexibility to describe the open-shell singlet species. In recent years, an accurate description of spin splittings and exchange couplings has become an important area in molecular magnetism. For systems with only two spin centers and one electron per center, we can model the exchange coupling as a singlet-triplet splitting ( $J = E_S - E_T$ ). We perform computations on a copper oxylate compound denoted as CuOC and shown in Fig. 2.3[63]. Geometries were obtained via the supplementary information of Ref 63. We used both the def2-SVP and the def2-TZVP basis sets.[64] The two singly occupied orbitals were used for our active space. We used 8 OpenMP threads per MPI process.

For def2-SVP, we performed a series of computations from 8 cores to 1024 cores. We notice that the timings for def2-SVP become too small to get reliable speedups once you reach 1024 cores. This is mainly due to the size of the problem. However, we still show 66 percent efficiency with 1024 cores. Fig. 2.4 shows the speed-ups from 8 cores to 1024 cores and Table 2.2 shows the overall timings for the CASSCF procedure. At 1024 cores, the entire CASSCF procedure takes about 222 s of wall time. With the def2-TZVP, we can still attain 56 percent efficiency with 2048 cores. A major limitation of our program is that only the Fock build is parallel, so we are not able to speed-up any of the linear algebra and other potentially computational expensive steps. This leads to some limitation on the scalability. However, the entire CASSCF procedure requires 1253 s of wall time. The spin splittings of CuOC are obtained in less than an hour with both the def2-SVP and def-TZVP basis sets. We obtained  $J$  values of  $-8.2 \text{ cm}^{-1}$  and  $-8.7 \text{ cm}^{-1}$  for the def2-SVP and def2-TZVP basis sets and the experimentally value is  $-37.0 \text{ cm}^{-1}$ .

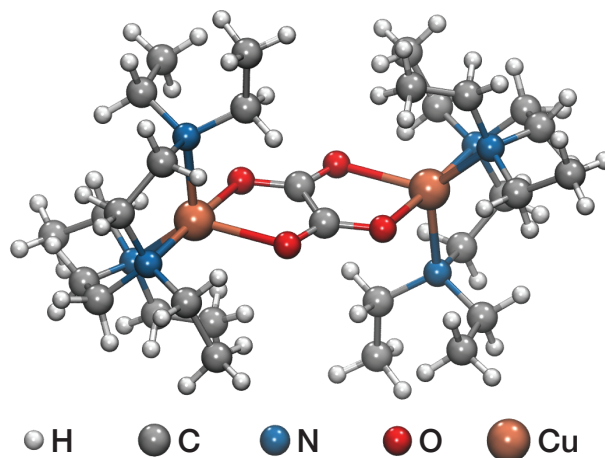


Figure 2.3: A large transition metal complex used as a test set for computing spin splittings. The molecule is a Copper oxalate compound.

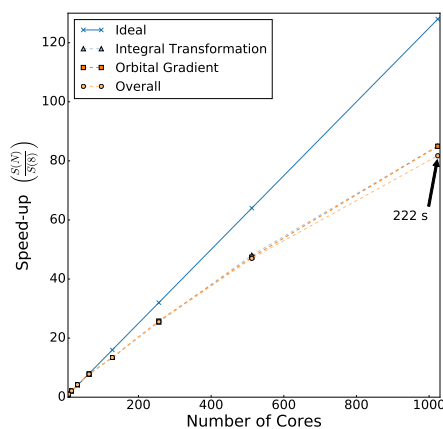


Figure 2.4: Speed-ups for the integral transformation, orbital gradient, and the overall iteration for CuOC. A def2-SVP basis set with 970 basis functions was used. All speed-ups were done relative to 8 cores. The value on the graph represents the overall time for 1024 cores.

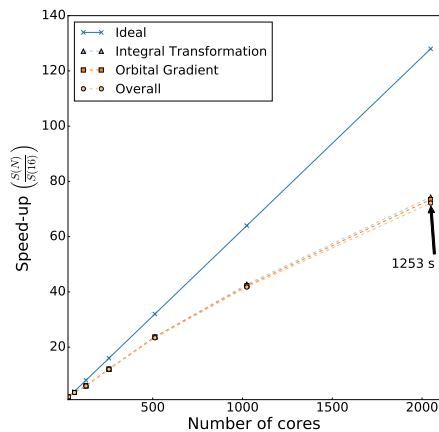


Figure 2.5: Speed-ups for the integral transformation, orbital gradient, and the overall iteration for CuOC. A def2-TZVP basis set with 1726 basis functions was used. All speed-ups of computed relative to 16 cores. The value on the graph represents the overall time for 2048 cores.

Table 2.2: Speed-ups, efficiencies, and overall for CASSCF computation with both the def2-SVP and def2-TZVP basis sets. Overall timing corresponds to the the entire CASSCF procedure. Speed-up is defined as  $\frac{S(N)}{S(8)}$  for def2-SVP and  $\frac{S(N)}{S(16)}$  for def2-TZVP.

Basis	Cores	Overall Timing	Speed-up	Efficiency
Def-SVP	8	18143.00	1.00	1.00
	16	8443	2.15	1.07
	32	4279	4.24	1.06
	64	2319	7.82	0.98
	128	1350	13.44	0.84
	256	711	25.52	0.80
	512	386	47.00	0.73
	1024	222	81.73	0.64
Def-TZVP	16	90418	1.00	1.00
	32	45271	2.00	1.00
	64	25235	3.58	0.90
	128	15189	5.95	0.74
	256	7534	12.00	0.75
	512	3864	23.40	0.73
	1024	2165	41.76	0.65
	2048	1253	73.45	0.56

### 2.3.3 Polycarbene

In this section, we demonstrate the scalability of the subgroup algorithm on a polycarbene molecule with a STO-3G basis set. We used this basis set as it demonstrates what will happen to our algorithm once communication becomes a bottleneck. Our algorithm requires a user defined entry of how many densities will be given to each subgroup or processors. A density group number of 5 corresponds to 11 densities per processor group. The number of densities is computed as  $N_A(N_A + 1)/2$ , so for 10 active orbitals, we have 55 densities. We test a density group number of both 5 and 11. We choose to use 440, 880, 1320, 1760, and 2220 cores as a test. These cores were chosen to make it possible to compare results between the different size density groups. For a density group of 5, the number of processors per density group is defined as the number of processors divided by the density group. We also compare the against the normal algorithm which is denoted as DG 1.

Table 2.3 presents timings for the various different density subgroups. For the normal algorithm, the communication of GTFock starts to become the major bottleneck. At 880 cores, the integral transform reaches a minimum of 1.56 seconds, but as the number of cores increases, the integral transformation starts to increase. This is primarily due to the increase of communication. By allowing multiple densities to be processed in parallel, we notice that the integral transformation decreases thus allowing our integral transformation to scale with more cores. For 2220 cores, we achieve nearly 4 times the speed-up relative to the normal algorithm. The major reason for this speed-up is due to the reduced communication by using processor subgroups. Processor subgroups allow one to split the MPI communicators into separate groups. By splitting the communicators, the number of cores present in each communicator decreases leading to lower communication time. This algorithm benefits from this reduced communication only when communication starts to become a bottleneck. The lower basis set allows this behavior to appear when using much fewer cores. A larger basis set would scale for more cores, but eventually, communication would start to dominate.

Table 2.3: The performance of the DG algorithm for polycarbene with a density group of 1, 5, and 11, respectively. The timings are for one integral transformation.

Cores	Density Groups timings (s)		
	1	5	11
440	1.70	1.34	1.73
880	1.56	0.79	0.94
1320	1.61	0.63	0.72
1760	1.87	0.54	0.55
2220	2.25	0.52	0.49

## 2.4 Conclusion

In this work, we introduce an MPI/OpenMP implementation of the AO-CASSCF. The major bottlenecks of CASSCF can be formulated as a series of generalized Coulomb- and exchange-like builds. By using the Fock builder, GTFock, we were

able to implement a parallel CASSCF algorithm. We also demonstrate that we are able to run up to 2048 cores with at least 60 percent efficiency in some cases. We also introduced a new algorithm for potential benefit for use in developing Parallel CASSCF algorithms for large active spaces.

## 2.5 Acknowledgments

This material is based upon work supported by the U.S. Department of Energy, Office of Science, Office of Workforce Development for Teachers and Scientists, Office of Science Graduate Student Research (SCGSR) program. The SCGSR program is administered by the Oak Ridge Institute for Science and Education for the DOE under contract number DESC0014664. This work was also partially supported via Emory start up funds. (A portion of) The research was performed using EMSL, a DOE Office of Science User Facility sponsored by the Office of Biological and Environmental Research. (Part of ) The work described in this article was performed by Pacific Northwest National Laboratory, which is operated by Battelle for the United States Department of Energy under Contract DE-AC05-76RL01830.

## 2.6 Appendix

In this section, for the MO indexing, we will use the following notation:  $i, j$  for core orbitals;  $a, b$  for virtual orbitals;  $u, v, x, y$  for active orbitals; and  $p, q, r$  for general molecular orbitals. The notation  $\mu, \rho, \sigma$ , and  $\tau$  correspond to atomic orbitals.  $\Phi$  corresponds to a slater determinant indexed with  $I$ .  $\hat{E}$  corresponds to a spin-free excitation operator.

The wavefunction for CASSCF is parameterized as follows,

$$|\Psi_{\text{CASSCF}}\rangle = \sum_I e^{-\hat{\kappa}} c_I |\Phi_I\rangle, \quad (2.12)$$

where  $c_I$  is the CI coefficients obtained via solution of the CI step and  $\hat{\kappa}$  is the orbital

rotation operator,

$$\hat{\kappa} = \sum_{p < q} \kappa_{pq} (\hat{E}_{pq} - \hat{E}_{qp}), \quad (2.13)$$

and  $\hat{E}_{pq}$  are the spin-free excitation operators. Solving both the CI coefficients and orbital rotations is done via a Newton-Rhapson approach,

$$E^{(2)} = E_0 + \kappa_{pq}^T g_{pq} + \kappa_{pq}^T h_{pq,rs} \kappa_{pq} \quad (2.14)$$

$$g_{pq} = \langle 0 | [\hat{H}, \hat{E}_{pq} - \hat{E}_{qp}] | 0 \rangle \quad (2.15)$$

$$h_{pq,rs} = \langle 0 | [ [\hat{E}_{pq} - \hat{E}_{qp}, \hat{H}], \hat{E}_{pq} - \hat{E}_{qp} ] | 0 \rangle \quad (2.16)$$

$$\kappa_{pq}^i = \kappa_{pq}^{i-1} - h_{pq,rs}^{-1} g_{rs} \quad (2.17)$$

At convergence, the orbital gradient must be equal to zero. The computation of the orbital gradient is directly related to the computation of the CASSCF Fock matrix,

$$g_{pq} = F_{pq} - F_{qp}, \quad (2.18)$$

$$F_{pq} = \gamma_{pm} h_{qm} + \Gamma_{puxy}(qu|xy). \quad (2.19)$$

Obtaining efficient implementations of CASSCF involves taking advantage of the sparsity of both the one particle density matrix ( $\gamma$  and  $\Gamma$ ),

$$\gamma_{pq} = \sum_{IJ} c_I c_J \langle \Phi_I | \hat{E}_{pq} | \Phi_J \rangle, \quad (2.20)$$

$$\Gamma_{pqrs} = \frac{1}{2} \sum_I \sum_J \langle \Phi_I | \hat{E}_{pq} \hat{E}_{rs} - \delta_{qr} \hat{E}_{ps} | \Phi_J \rangle. \quad (2.21)$$

The orbital gradient can be computed from the inactive Fock matrix ( ${}^I F_{pq}$ ) and the active Fock matrix ( ${}^A F_{pq}$ ),

$${}^I F_{pq} = h_{pq} + 2(pq|rs) - (ps|rq), \quad (2.22)$$

$${}^A F_{pq} = \gamma_{ux} \left[ (pq|ux) - \frac{1}{2}(px|uq) \right]. \quad (2.23)$$

Using these intermediates, the CASSCF Fock matrix can be computed quite effi-

ciently,

$$F_{mp} = 2^I F_{pm} + 2^A F_{pm} \quad (2.24)$$

$$F_{up} = \sum_w^I F_{pw} \gamma_{uw} + \sum_{uxy} \Gamma_{tuxy}(pu|xy) \quad (2.25)$$

$$F_{en} = 0 \quad (2.26)$$

The nonredundant contributions to the diagonal hessian approximation is,[\[52\]](#)

$$h_{mm,ee} = 4(I F_{ee} + A F_{ee} - I F_{ii} - A F_{ee}) \quad (2.27)$$

$$h_{uu,ee} = 2\gamma_{uu}(I F_{ee} + A F_{aa}) \quad (2.28)$$

$$\begin{aligned} & -2.0 \left( \sum_p^I F_{p,u} \gamma_{tu} + \sum_p (pu|xy) \Gamma_{tuxy} \right) \\ h_{ii,uu} &= 4.0(I F_{uu} + A F_{uu}) + 2\gamma_{uu} I F_{ii} + 2\gamma_{uu} A F_{ii} \\ & -4(I F_{ii} + A F_{ii}) + 2 \left( \sum_p^I F_{p,u} \gamma_{tu} + \sum_p (pu|xy) \Gamma_{tuxy} \right) \end{aligned} \quad (2.29)$$

With both the orbital gradient and the diagonal hessian formed, the rotation operator can be formed.

$$\hat{K}_{pq} = e^{-\hat{\kappa}} \quad (2.30)$$

$$C_{\sigma p}^{i+1} = C_{\sigma q}^{(0)} \hat{K}_{pq} \quad (2.31)$$

Evaluating the matrix exponential is done via Taylor expansion and through a scaling and squaring method.[\[65, 66\]](#) The Taylor expansion is expanded to third order and then the columns are reorthogonalized via a gram-schmidt procedure. We found that the gram-schmidt procedure became a bottleneck for large number of basis functions, so we also implemented the scaling and squaring method. We found that the scaling and squaring method was faster than the Taylor series, so all of our timings are presented with the scaling and squaring method. It is important to state that for a truly scalable CASSCF algorithm one would need to implement a parallel algorithm for the evaluating of this matrix exponential.

# Chapter 3 An integral-factorized implementation of the driven similarity renormalization group second-order multireference perturbation theory

## 3.1 Introduction

Second-order Møller–Plesset perturbation theory (MP2) is perhaps one of the simplest approaches to treat *dynamic* electron correlation in atoms and molecules.[67] Efficient implementations of MP2 may be achieved via techniques that factorize the two-electron integrals such as density fitting (DF)[68, 69] or Cholesky decomposition (CD).[70–75] Due to lower storage requirements, integral factorization techniques significantly reduce the cost of MP2 calculations and easily permit to target systems with 2000–3000 basis functions.[76] Linear scaling[76–79] and stochastic[80–82] implementations of MP2 can further reduce the asymptotic computational scaling of MP2 from  $\mathcal{O}(N^5)$  to  $\mathcal{O}(N)$ , where  $N$  is the number of basis functions.

However, when MP2 is applied to study open-shell species, the buildup of *static* correlation due to near-degenerate excitation configurations can lead to the divergence of the correlation energy. In this case, it is necessary to use a *multireference* generalization of perturbation theory (MRPT) that can handle both *dynamic* and *static* correlation effects. In practice, the distinction between *dynamic* and *static* correlation is enforced by dividing the full configuration interaction space into a reference space and its orthogonal complement. The reference space consists of determinants generated by varying the occupation of the close-lying active orbitals, and consequently captures static correlation effects. Numerous multireference perturbation theories have been proposed,[83–89] many of which have been conveniently reviewed and compared in

Refs. 87 and 88.

A troubling aspect of several multireference perturbation theories is the well-known intruder-state problem.[90] Intruder states are encountered when determinants that lie within the reference space become near-degenerate with determinants that lie in the orthogonal complement. In perturbative theories, intruders lead to divergences in the first-order amplitudes, and the corresponding potential energy curves show characteristic spikes.[91–93] A popular solution to remove intruders is shifting the energy denominators.[94] However, level shifting can significantly affect computed spectroscopic constants[95] and the order of electronic states.[96] In the second-order  $n$ -electron valence state perturbation theory (NEVPT2),[86, 97, 98] intruders are removed by using Dyal’s modified zeroth-order Hamiltonian.[99] Nevertheless, Zgid et al.[100] noticed that if the three- and four-particle density cumulants are approximated then “false intruders” may also appear in NEVPT2.

The importance of the intruder-state problem is not limited to multireference perturbation theories. In the case of multireference coupled cluster theories (MRCC)[101–110] and other nonperturbative theories of dynamical correlation,[111–113] intruders cause numerical instability problems. In this case, however, it is more appropriate talk of *intruder solutions*, which arise from existence of multiple solutions to the MRCC equations.[92] Unfortunately, it is still not clear whether or not traditional techniques used to remove intruders in MRPT can be extended to the case of nonperturbative multireference methods. Therefore, finding a solution to the problem of intruders in MRPT might also shed light on how to create highly-accurate multireference approaches that are numerically stable.

Recently, we have proposed the driven similarity renormalization group (DSRG),[114] a many-body formalism inspired by flow renormalization group methods.[115–121] The DSRG was used to formulate a theory of dynamic electron correlation that is free from divergences due to vanishing denominators. In the unitary DSRG ansatz,

the bare Hamiltonian ( $\hat{H}$ ) is progressively brought to a block-diagonal form (renormalized) via a continuous unitary transformation [ $\hat{U}(s)$ ] controlled by the so-called flow variable  $s$ :

$$\hat{H} \rightarrow \bar{H}(s) = \hat{U}(s)\hat{H}\hat{U}^\dagger(s), \quad s \in [0, \infty). \quad (3.1)$$

In the limit  $s \rightarrow \infty$  the DSRG unitary operator  $\hat{U}(s)$  is required to block-diagonalize the Hamiltonian. More specifically, if we indicate the non-diagonal part of  $\bar{H}(s)$  with  $[\bar{H}(s)]_N$ ,[\[122, 123\]](#) then we require that in the limit of  $s$  that goes to infinity, the DSRG transformation must zero the nondiagonal parts of  $\bar{H}(s)$ , that is  $\lim_{s \rightarrow \infty} [\bar{H}(s)]_N = 0$ . For intermediate values of  $s$ , the DSRG transformation achieves a partial block-diagonalization of the Hamiltonian, leaving states that differ in energy by less than the energy cutoff  $\Lambda = s^{-1/2}$  mostly unchanged.[\[115, 124–126\]](#) Consequently, in the DSRG the mixing of reference-space determinants with close-lying determinants in the orthogonal complement is suppressed and intruder states are avoided.

Another distinctive aspect of the DSRG is that it employs a Fock-space many-body formalism,[\[127, 128\]](#) such that Eq. (3.1) should be interpreted as a set of operator equations. Nooijen and coworkers[\[107\]](#) recently pointed out that a many-body formulation of multireference theories is advantageous because it removes the need to orthogonalize the excitation manifold. The orthogonalization step is often a bottleneck that prevents computations with large active spaces. For example, in a study of the complete active space perturbation theory (CASPT2)[\[83, 129–131\]](#) coupled with the density matrix renormalization group (DMRG),[\[54, 58, 132, 133\]](#) Yanai and Kurashige [\[134\]](#) found that the perturbation theory is limited to approximately 30 active orbitals per irreducible representation due to the required diagonalization of the overlap metric between internally-contracted configurations.

In a previous work,[\[135\]](#) we formally extended the DSRG to multireference cases (MR-DSRG) by employing the generalized Wick theorem of Mukherjee and Kutzelnigg.[\[136\]](#) To study the viability of the MR-DSRG approach we performed a perturbative anal-

ysis and derived a second-order MR-DSRG perturbation theory (DSRG-MRPT2). The DSRG-MRPT2 energy and amplitude equations are surprisingly simple and lead to a computational approach that requires at most the three-body cumulant of the reference wave function. Benchmark computations on small systems (HF, N<sub>2</sub>, and *p*-benzyne) showed that the DSRG-MRPT2 has an accuracy comparable to that of other second-order MRPTs. The DSRG-MRPT2 method avoids the intruder-state problem without the use of level-shifting or increasing the size of the active space. In addition, it is rigorously size consistent,[\[137, 138\]](#) and thus applicable to large systems.

The present work focuses on the efficient implementation of the DSRG-MRPT2 theory to extend its applicability to chemically interesting systems. We carefully analyze each energy contribution, and realize the possibility to factorize some terms by taking advantage of the structure of the one-particle and one-hole density matrices. In most common applications, the cost of the improved algorithm is comparable to that of MP2. The simplicity of the DSRG-MRPT2 equations allows us to utilize common integral factorization techniques,[\[139\]](#) including density fitting and Cholesky decomposition, to reduce the memory and disk requirements. In addition to MP2, various electronic structure methods have benefited from these integral factorization tactics.[\[76, 140–145\]](#) For instance, the Cholesky-decomposed CASPT2 has been applied to systems with up to 1500 basis functions[\[146, 147\]](#) and the density-fitted NEVPT2 has been used in applications with up to 2000 basis functions.[\[97, 148\]](#)

This paper proceeds as follow. In Sec. II, we start with an overview of the DSRG-MRPT2 theory and integral factorization techniques. Then, in Sec. III we analyze the computational complexity of each energy term and detail our current implementation. Section V presents applications of DSRG-MRPT2 to evaluate the singlet-triplet splittings of naphthynes. Finally, we discuss future developments of the DSRG-MRPT2.

## 3.2 Theory

### 3.2.1 The MR-DSRG formalism

In this section we briefly summarize the MR-DSRG approach.[135] We assume that the reference is defined by a set of spin orbitals  $\phi^p$  partitioned into core (**C**), active (**A**), and virtual (**V**) subsets of size  $N_{\mathbf{C}}$ ,  $N_{\mathbf{A}}$ , and  $N_{\mathbf{V}}$ , respectively. Core orbitals are designated by indices  $m, n$ , active orbitals by indices  $u, v, w, x, y, z$ , and virtual orbitals by indices  $e, f$ . We also introduce two composite orbital subsets: hole (**H** = **C**  $\cup$  **A**) and particle (**P** = **V**  $\cup$  **A**) of dimension  $N_{\mathbf{H}} = N_{\mathbf{C}} + N_{\mathbf{A}}$  and  $N_{\mathbf{P}} = N_{\mathbf{V}} + N_{\mathbf{A}}$ , respectively. Orbitals belonging to hole set are associated with the labels  $i, j, k, l$ , while particle orbitals are labeled with  $a, b, c, d$ . General orbitals (hole or particle) are labeled as  $p, q, r, s$ .

We consider the case of a complete active space (CAS) self-consistent field (CASSCF) or a CAS configuration interaction (CASCI) reference wave function  $\Phi$  obtained by doubly occupying the core orbitals and distributing a given number of active electrons ( $n_{\text{act}}$ ) in the active orbitals [CAS( $n_{\text{act}}$ ,  $N_{\mathbf{A}}$ )]. The reference  $\Phi$  defines the Fermi vacuum with respect to which all operators are normal ordered according to Mukherjee and Kutzelnigg's generalized Wick theorem.[136, 149–153] From the reference wave function we also extract the one-particle density matrix ( $\gamma_p^q$ ) as well as the two- and three-body cumulants ( $\lambda_{uv}^{xy}$ ,  $\lambda_{uvw}^{xyz}$ ),[136, 154, 155] defined as:

$$\gamma_q^p = \langle \Phi | \hat{a}_p^\dagger \hat{a}_q | \Phi \rangle, \quad (3.2)$$

$$\lambda_{uv}^{xy} = \gamma_{uv}^{xy} - \gamma_u^x \gamma_v^y + \gamma_u^y \gamma_v^x, \quad (3.3)$$

$$\lambda_{uvw}^{xyz} = \gamma_{uvw}^{xyz} - \sum_{\pi} (-1)^{\pi} \gamma_u^x \lambda_{vw}^{yz} - \det(\gamma_u^x \gamma_v^y \gamma_w^z), \quad (3.4)$$

where  $\hat{a}_p^\dagger$  ( $\hat{a}_q$ ) is a second-quantized creation (annihilation) operator, while  $\gamma_{uv}^{xy} = \langle \Phi | \hat{a}_x^\dagger \hat{a}_y^\dagger \hat{a}_v \hat{a}_u | \Phi \rangle$  and  $\gamma_{uvw}^{xyz} = \langle \Phi | \hat{a}_x^\dagger \hat{a}_y^\dagger \hat{a}_z^\dagger \hat{a}_w \hat{a}_v \hat{a}_u | \Phi \rangle$  are the reference two- and three-particle density matrices, respectively. In Eq. (3.4)  $\det(\cdot)$  indicates the sum of all permutations of lower labels with a sign factor corresponding to the parity of permu-

tations and  $\sum(-1)^\pi$  indicates a sum over all permutations of the lower and upper labels with a sign factor corresponding to the parity of a given permutation. Note that for a CASSCF/CASCI reference the cumulants are null unless all indices belong to the active space. For convenience we also define the one-body cumulant as  $\lambda_u^v = \gamma_u^v$ , with  $u, v \in \mathbf{A}$ . The MR-DSRG equations for the amplitude and energy  $[E(s)]$  are given by:

$$E(s) = \langle \Phi | \bar{H}(s) | \Phi \rangle, \quad (3.5)$$

$$[\bar{H}(s)]_{\mathbf{N}} = \hat{R}(s), \quad (3.6)$$

where  $\hat{R}(s)$  is the source operator, a  $s$ -dependent Hermitian operator that drives the transformation of the Hamiltonian. Thus, the unitary operator,  $\hat{U}(s)$ , is implicitly defined by  $\hat{R}(s)$ . The unitary operator  $\hat{U}(s)$  that controls the DSRG transformation is expressed as the exponential of an anti-Hermitian operator  $\hat{A}(s)$ , that is,  $\hat{U}(s) = \exp[\hat{A}(s)]$ . The operator  $\hat{A}(s)$  is conveniently expressed in terms of the coupled cluster excitation operator  $\hat{T}(s)$ , so that  $\hat{A}(s) = \hat{T}(s) - \hat{T}^\dagger(s)$ . Note that internal amplitudes that involve only active-orbital indices are excluded from  $\hat{T}(s)$ , that is  $t_{uv\dots}^{xy\dots}(s) = 0 \forall u, v, x, y \dots \in \mathbf{A}$ .

### 3.2.2 The DSRG-MRPT2 method

The starting point of the DSRG-MRPT2 approach is the partitioning of the normal-ordered Hamiltonian into a zeroth-order part  $[\hat{H}^{(0)}]$  plus a first-order perturbation  $[\hat{H}^{(1)}]$ . The zeroth-order Hamiltonian is chosen to contain the reference energy ( $E_0$ ) and the diagonal block of the one-body operator  $[\hat{F}^{(0)}]$ :[\[135\]](#)

$$\hat{H}^{(0)} = E_0 + \hat{F}^{(0)}, \quad (3.7)$$

$$\hat{F}^{(0)} = \sum_p \varepsilon_p \{\hat{a}_p^p\}, \quad (3.8)$$

where the orbital energies  $\varepsilon_p = f_p^p$  are the diagonal elements of the generalized Fock matrix:

$$f_p^q = h_p^q + \sum_{rs} v_{pr}^{qs} \gamma_s^r. \quad (3.9)$$

The quantities  $h_p^q = \langle \phi_p | \hat{h} | \phi^q \rangle$  and  $v_{pq}^{rs} = \langle \phi_p \phi_q | | \phi^r \phi^s \rangle$  are respectively one-electron and antisymmetrized two-electron integrals in the molecular orbital (MO) basis.

As is the case for other perturbation theories, we find it advantageous to formulate the DSRG-MRPT2 in a basis of semicanonical molecular orbitals[156] so that the core, active, and virtual blocks of the generalized Fock matrix are diagonal. This choice implies that  $\hat{F}^{(1)}$  only contains contributions from the off-diagonal blocks of the Fock matrix.

The DSRG-MRPT2 equations may be obtained from Eqs.(3.5) and (3.6) by performing an order-by-order expansion.[157] The zeroth-, first-, and second-order energy expressions are given by:[135]

$$E^{(0)}(s) = E_0, \quad (3.10)$$

$$E^{(1)}(s) = 0, \quad (3.11)$$

$$E^{(2)}(s) = \langle [\tilde{H}^{(1)}(s), \hat{T}^{(1)}(s)] \rangle, \quad (3.12)$$

where  $\tilde{H}^{(1)}$  is an effective first-order Hamiltonian with modified non-diagonal components:

$$\tilde{H}^{(1)}(s) = \hat{H}^{(1)}(s) + [\hat{R}^{(1)}(s)]_N, \quad (3.13)$$

while the diagonal components of  $\tilde{H}^{(1)}$  are identical to those of  $\hat{H}^{(1)}$ .

A first-order expansion of the MR-DSRG amplitude equations leads to the equation:

$$[\hat{H}^{(1)}]_N + [\hat{H}^{(0)}, \hat{T}^{(1)}]_N = [\hat{R}^{(1)}(s)]_N, \quad (3.14)$$

from which explicit equations for the first-order amplitudes can be derived:[135]

$$t_a^{i,(1)}(s) = [f_a^{i,(1)} + \sum_{ux}^{\mathbf{A}} \Delta_u^x t_{ax}^{iu,(1)}(s) \gamma_u^x] \frac{1 - e^{-s(\Delta_a^i)^2}}{\Delta_a^i}, \quad (3.15)$$

$$t_{ab}^{ij,(1)}(s) = v_{ab}^{ij,(1)} \frac{1 - e^{-s(\Delta_{ab}^{ij})^2}}{\Delta_{ab}^{ij}}. \quad (3.16)$$

Here we have introduced the Møller–Plesset denominators  $\Delta_{ab\dots}^{ij\dots}$ , defined as  $\Delta_{ab\dots}^{ij\dots} = \varepsilon_i + \varepsilon_j + \dots - \varepsilon_a - \varepsilon_b - \dots$ . In the derivation of Eqs. (3.15) and (3.16) we used the source operator introduced in Ref. 114, which is designed to reproduce the energy of the second-order similarity renormalization group.[158]

Once the first-order amplitudes are solved, the second-order energy  $E^{(2)}(s)$  can be obtained via an efficient non-iterative procedure that requires at most three-body density cumulants. For convenience, we list all DSRG-MRPT2 energy contributions in Table 3.1. These quantities are expressed in terms of the modified first-order Fock matrix:

$$\begin{aligned} \tilde{f}_a^{i,(1)}(s) &= f_a^{i,(1)} [1 + e^{-s(\Delta_a^i)^2}] \\ &+ \left[ \sum_{ux} \Delta_u^x t_{ax}^{iu,(1)}(s) \gamma_u^x \right] e^{-s(\Delta_a^i)^2}, \end{aligned} \quad (3.17)$$

the modified two-electron integrals:

$$\tilde{v}_{ab}^{ij,(1)}(s) = v_{ab}^{ij,(1)} [1 + e^{-s(\Delta_{ab}^{ij})^2}], \quad (3.18)$$

the one-particle and one-hole density matrix elements ( $\gamma_q^p, \eta_q^p = \delta_q^p - \gamma_q^p$ ), and the two- and three-body density cumulants ( $\lambda_{xy}^{uv}, \lambda_{xyz}^{uvw}$ ) of the reference  $\Phi$ . Eqs. (3.15)–(3.18) and the equations reported in Table 3.1 define the DSRG-MRPT2 method.

To highlight the mechanism by which the DSRG-MRPT2 avoids intruders, we perform a Maclaurin expansion of the first-order amplitudes as a function of the energy denominators. For example, the  $t_2$  amplitude [Eq. (3.16)] can be rewritten as:

$$t_{ab}^{ij,(1)}(s) = v_{ab}^{ij,(1)} \left( s \Delta_{ab}^{ij} + \mathcal{O}[s^{3/2}(\Delta_{ab}^{ij})^3] \right), \quad (3.19)$$

Table 3.1: DSRG-MRPT2 energy contributions. Following the Einstein convention, summation over repeated indices is assumed. Asymptotic cost scalings are given in big  $\mathcal{O}$  notation.

Term	Energy Expression	Cost
	$\langle [\tilde{F}^{(1)}(s), \hat{T}_1^{(1)}(s)] \rangle$	
A	$+ \tilde{f}_j^{b,(1)}(s) t_a^{i,(1)}(s) \gamma_i^j \eta_b^a$	$N_P^2 N_H^2$
	$\langle [\tilde{V}^{(1)}(s), \hat{T}_1^{(1)}(s)] \rangle$	
B	$+ \frac{1}{2} \tilde{v}_{xy}^{ev,(1)}(s) t_e^{u,(1)}(s) \lambda_{uv}^{xy}$	$N_A^4 N_V$
C	$- \frac{1}{2} \tilde{v}_{my}^{uv,(1)}(s) t_x^{m,(1)}(s) \lambda_{uv}^{xy}$	$N_A^4 N_C$
	$\langle [\tilde{F}^{(1)}(s), \hat{T}_2^{(1)}(s)] \rangle$	
D	$+ \frac{1}{2} \tilde{f}_x^{e,(1)}(s) t_{ey}^{uv,(1)}(s) \lambda_{uv}^{xy}$	$N_A^4 N_V$
E	$- \frac{1}{2} \tilde{f}_m^{v,(1)}(s) t_{xy}^{um,(1)}(s) \lambda_{uv}^{xy}$	$N_A^4 N_C$
	$\langle [\tilde{V}^{(1)}(s), \hat{T}_2^{(1)}(s)] \rangle$	
F	$+ \frac{1}{4} \tilde{v}_{kl}^{cd,(1)}(s) t_{ab}^{ij,(1)}(s) \gamma_i^k \gamma_j^l \eta_c^a \eta_d^b$	$N_P^3 N_H^2$
G	$+ \frac{1}{8} \tilde{v}_{xy}^{cd,(1)}(s) t_{ab}^{uv,(1)}(s) \eta_c^a \eta_d^b \lambda_{uv}^{xy}$	$N_A^4 N_P^2$
H	$+ \frac{1}{8} \tilde{v}_{kl}^{uv,(1)}(s) t_{xy}^{ij,(1)}(s) \gamma_i^k \gamma_j^l \lambda_{uv}^{xy}$	$N_A^4 N_H^2$
I	$+ \tilde{v}_{jx}^{bu,(1)}(s) t_{ay}^{iv,(1)}(s) \gamma_i^j \eta_b^a \lambda_{uv}^{xy}$	$N_A^4 N_P N_H$
J	$+ \frac{1}{4} \tilde{v}_{mz}^{uv,(1)}(s) t_{xy}^{mw,(1)}(s) \lambda_{uvw}^{xyz}$	$N_A^6 N_C$
K	$+ \frac{1}{4} \tilde{v}_{xy}^{we,(1)}(s) t_{ez}^{uv,(1)}(s) \lambda_{uvw}^{xyz}$	$N_A^6 N_V$

which approaches zero in the limit of  $|\Delta_{ab}^{ij}| \rightarrow 0$ . Thus for finite values of  $s$ , the second-order energy,  $E^{(2)}(s)$ , is well-behaved and free from divergences due to small energy denominators. One of the drawbacks of the DSRG-MRPT2 renormalization procedure is that the final energy shows a dependence on the value of  $s$  used in a computation. In our previous work, [135] we analyzed the  $s$ -dependence of the DSRG-MRPT2 energy and found that the range  $s \in [0.1, 1.0]$   $E_h^{-2}$  gives the best agreement with full configuration interaction results. Values of  $s$  that fall out of this ‘‘Goldilocks zone’’ either lead to recovering too little correlation energy (when  $s \ll 0.1$ ) or expose the theory to intruders (when  $s \gg 1$ ).

### 3.2.3 Integral factorizations

The simple structure of the MR-DSRG amplitude and energy equations (Table 3.1) allows the use of integral factorization techniques such as DF and/or Cholesky de-

composition to improve the efficiency of the DSRG-MRPT2. Integral factorization techniques seek to approximate the electron repulsion integrals as a contraction of two three-index tensors. The two-electron integrals written in chemist’s notation can be factorized as:

$$(pq|rs) \approx \sum_Q^M B_{pq}^Q B_{rs}^Q, \quad (3.20)$$

where  $M$  is the size of the auxiliary basis set ( $\chi_P(\mathbf{r})$ ). In the DF approach, the factors  $B_{pq}^Q$  are given by:[41]

$$B_{pq}^Q = \sum_P (pq|P) [\mathbf{J}^{-1/2}]_{PQ}, \quad (3.21)$$

where  $(pq|P)$  and  $J_{PQ}$  are three- and two-center integrals defined as:

$$(pq|P) = \int d\mathbf{r}_1 \int d\mathbf{r}_2 \phi_p(\mathbf{r}_1) \phi_q(\mathbf{r}_1) r_{12}^{-1} \chi_P(\mathbf{r}_2), \quad (3.22)$$

$$J_{PQ} = \int d\mathbf{r}_1 \int d\mathbf{r}_2 \chi_P(\mathbf{r}_1) r_{12}^{-1} \chi_Q(\mathbf{r}_2). \quad (3.23)$$

In this work we evaluate the DSRG-MRPT2 energy using the resolution of the identity (RI) basis sets of Weigend and co-workers.[159] We note, however, that there is no consensus on the most appropriate auxiliary basis set for multireference perturbation theories.

In the CD approach, the factors  $B_{pq}^Q$  are obtained directly via numerical Cholesky decomposition[65] of the four-index two-electron integrals.[72–74] The upper bound of the summation  $M$  in Eq. (3.20) is determined by a CD threshold, which measures the error introduced by the Cholesky decomposition.[73, 74]

### 3.3 Implementation

An efficient implementation of the DSRG-MRPT2 is achieved by taking advantage of the structure of the density matrices and integral factorization. In most practically relevant cases, the number of active orbitals is negligible compared to the number of

$$\gamma_q^p = \begin{cases} \delta_q^p & p, q \in \mathbf{C} \\ \lambda_q^p & p, q \in \mathbf{A} \\ 0 & \text{otherwise} \end{cases} \quad \begin{array}{c} \mathbf{C} \\ \mathbf{A} \\ \mathbf{V} \end{array} \begin{array}{|c|c|c|} \hline \text{red diagonal} & & \\ \hline & \text{red square} & \\ \hline & & \\ \hline \end{array}$$

$$\eta_q^p = \begin{cases} 0 & \text{otherwise} \\ \delta_q^p - \lambda_q^p & p, q \in \mathbf{A} \\ \delta_q^p & p, q \in \mathbf{V} \end{cases} \quad \begin{array}{c} \mathbf{C} \\ \mathbf{A} \\ \mathbf{V} \end{array} \begin{array}{|c|c|c|} \hline & & \\ \hline & \text{blue square} & \\ \hline & & \text{blue diagonal} \\ \hline \end{array}$$

Figure 3.1: The structures of one-particle density matrix  $\gamma_q^p$  and one-hole density matrix  $\eta_q^p$ . Non-zero elements of the one-particle and one-hole density matrices are indicated respectively in red and blue.

core and virtual orbitals, that is we may assume that:

$$N_{\mathbf{A}} \ll N_{\mathbf{C}} < N_{\mathbf{V}}. \quad (3.24)$$

Under this assumption, the most expensive term in the evaluation of the DSRG-MRPT2 energy is term F of Table 3.1. This term originates from the contraction  $\langle [\tilde{V}^{(1)}(s), \hat{T}_2^{(1)}(s)] \rangle$  and is given by:

$$F = \frac{1}{4} \sum_{ijkl}^{\mathbf{H}} \sum_{abcd}^{\mathbf{P}} \tilde{v}_{kl}^{cd,(1)}(s) t_{ab}^{ij,(1)}(s) \gamma_i^k \gamma_j^l \eta_c^a \eta_d^b. \quad (3.25)$$

After factorization into intermediate tensors, the computational cost required to evaluate term F scales as  $\mathcal{O}(N_{\mathbf{P}}^3 N_{\mathbf{H}}^2)$ .

For a CASSCF/CASCI reference, we can reduce the cost of evaluating term F by taking advantage of the structure of the one-particle and one-hole density matrices. As illustrated in Fig. 3.1,  $\gamma_q^p$  is diagonal in the core-core block, and in the active-active block it is equal to the one-body cumulant  $\lambda_q^p$ . Upon explicit replacement of the one-body density and hole density matrices into Eq. (3.25) we obtain eight contributions (F1–F8) that are reported in Table 3.2. Each term is also represented as a diagram in which one or more lines pass through a one-particle (red circle) or one-hole (blue circle) vertex. The most expensive contributions to term F [Eq. (3.25)] is diagram F1,

Table 3.2: DSRG-MRPT2 energy terms that arise from diagram F after taking into account the block structure of the one-hole and one-particle density matrices. Contractions involving the one-particle density matrix ( $\gamma_j^i$ ) and hole indices are indicated with a red circle, while contractions of the one-hole density matrix ( $\eta_b^a$ ) and particle indices are indicated with a blue circle.

Term	Diagram	Expression
F1		$\frac{1}{4} \sum_{mnef} \tilde{v}_{mn}^{ef,(1)}(s) t_{ef}^{mn,(1)}(s)$
F2		$\frac{1}{2} \sum_{mefuv} \tilde{v}_{mu}^{ef,(1)}(s) t_{ef}^{mv,(1)}(s) \gamma_v^u$
F3		$\frac{1}{2} \sum_{mneuw} \tilde{v}_{mn}^{ev,(1)}(s) t_{eu}^{mn,(1)}(s) \eta_v^u$
F4		$\frac{1}{4} \sum_{ef} \sum_{uvxy} \tilde{v}_{xu}^{ef,(1)}(s) t_{ef}^{yv,(1)}(s) \gamma_y^x \gamma_v^u$
F5		$\frac{1}{4} \sum_{mn} \sum_{uvxy} \tilde{v}_{mn}^{vy,(1)}(s) t_{ux}^{mn,(1)}(s) \eta_v^u \eta_y^x$
F6		$\sum_{me} \sum_{wvxy} \tilde{v}_{mx}^{ve,(1)}(s) t_{ue}^{my,(1)}(s) \gamma_y^x \eta_v^u$
F7		$\frac{1}{2} \sum_{wxyz} \sum_{evu} \tilde{v}_{yz}^{ve,(1)}(s) t_{ue}^{wx,(1)}(s) \gamma_w^y \gamma_x^z \eta_v^u$
F8		$\frac{1}{2} \sum_{mwz} \sum_{uvxy} \tilde{v}_{mw}^{vy,(1)}(s) t_{ux}^{mz,(1)}(s) \gamma_z^w \eta_v^u \eta_y^x$
		$\gamma_j^i$
		$\eta_b^a$

which has a computation scaling of  $\mathcal{O}(N_{\mathbf{V}}^2 N_{\mathbf{C}}^2)$ , followed by F2 and F3, which scale as  $\mathcal{O}(N_{\mathbf{V}}^2 N_{\mathbf{A}} N_{\mathbf{C}})$  and  $\mathcal{O}(N_{\mathbf{V}} N_{\mathbf{A}} N_{\mathbf{C}}^2)$ , respectively. The remaining diagrams shown in Table 3.2 (F4–F8) carry at least two active indices and are significantly less expensive to evaluate.

Diagram F1 may be written in a form that is reminiscent of the MP2 correlation energy:

$$\frac{1}{4} \sum_{mn}^{\mathbf{C}} \sum_{ef}^{\mathbf{V}} |v_{mn}^{ef}|^2 \frac{1 - e^{-2s(\Delta_{ef}^{mn})^2}}{\Delta_{ef}^{mn}}. \quad (3.26)$$

Eq. (3.26) can be implemented in an efficient way by an outer loop over pairs of occupied orbitals  $m$  and  $n$ . For each pair  $(m, n)$  we compute all the antisymmetrized

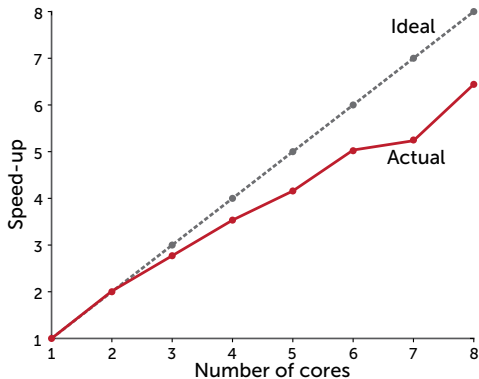


Figure 3.2: The scaling of diagram F1 of Table 3.2 for (2,3)-naphthylene using a cc-pVTZ basis set. The speed up is determined as  $\frac{S(1)}{S(N)}$  where  $S(i)$  is the total time required to evaluate this term using  $i$  threads. Results are for up to 8 threads on an Intel Xeon E5-2650 v2 processor.

two electron integrals ( $v_{mn}^{ef}, \forall e, f$ ) using the DF or CD factors. The integrals squared are then contracted with the renormalized denominators  $[1 - e^{-2s(\Delta_{ef}^{mn})^2}] / \Delta_{ef}^{mn}$  through a dot-product operation to give a pair energy for every  $m$  and  $n$ .[\[160\]](#) The loop over the  $(m, n)$  pairs is parallelized using OpenMP for shared memory architectures. The scaling of the implementation of Eq. (3.26) on a eight-core processor is demonstrated in Fig. 3.2. Our implementation is also optimized for the evaluation of diagrams F2 and F3 so that no storage of large four-index intermediate quantities is necessary.

The DSRG-MRPT2 equations are implemented in our code FORTE,[\[161\]](#) a suite of multireference methods written as a plugin to the PSI4 quantum chemistry package.[\[162\]](#) All tensor contractions were coded using the open-source library AMBIT.[\[163\]](#) AMBIT provides shared memory parallelization and performs tensor contractions using BLAS operations. A very convenient feature of AMBIT is its ability to deal with composite orbital spaces. Figure 3.3 gives an example of a tensor contraction encountered in the DSRG-MRPT2 equations and how it is implemented via AMBIT. Composite spaces are defined from “primitive” spaces (for example, the sets of core, active, virtual molecular orbitals) and arise naturally in all multireference theories based on a CASCI/CASSCF reference. AMBIT is aware of composite orbital spaces and can

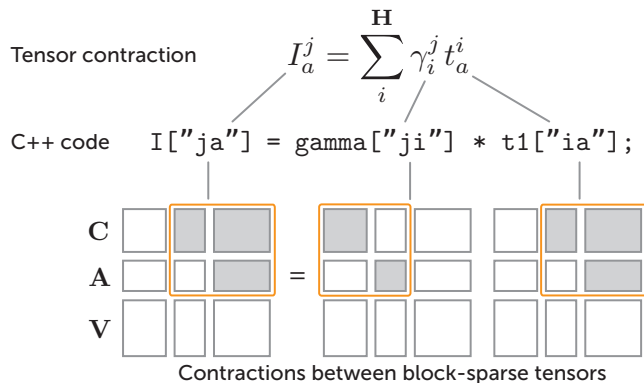


Figure 3.3: This figure illustrates the ability of the AMBIT tensor library to deal with block-sparse tensors that span composite orbital space. The tensor contraction shown at the top involves a summation over the index  $j$  that spans the generalized orbitals space ( $\mathbf{H}$ ), which is the union of the core ( $\mathbf{C}$ ) and active ( $\mathbf{A}$ ) orbitals. The tensors  $\gamma_i^j$  and  $t_a^i$  are defined over subsets (shown in orange) of the full orbital indices and are block sparse. For example, the  $\mathbf{A}$ - $\mathbf{A}$  block of  $t_a^i$  is zero because internal amplitudes are not defined in the DSRG-MRPT2. AMBIT allows to write contractions over block-sparse tensors as contractions over composite index tensors, thus, reducing the number of equations required to include in the source code.

perform contractions over block-sparse tensors. This feature greatly simplifies the implementation of multireference theories since it allows the user to directly encode tensor contractions that involve composite orbital indices.

In summary, the following procedure was used for computing the DSRG-MRPT2 energy using DF or CD integrals:

1. Compute  $\gamma_p^q$ ,  $\eta_p^q$ ,  $\lambda_{uv}^{xy}$ , and  $\lambda_{uvw}^{xyz}$  for the CASSCF/CASCI reference.
2. Compute the Fock matrix from  $\gamma_p^q$  and the DF/CD tensors.
3. Canonicalize the core, active, and virtual MOs.
4. Form the antisymmetrized two electron integrals with at least two active index from the DF/CD tensors.
5. Transform all the density matrices, cumulants, and integrals to the semi-canonical basis.
6. Compute the second order energy terms A–E, G–K, and F4–F8 using the AMBIT

library.

7. Compute the energy terms F1–F3 with an optimized algorithm that does not require storage of four-index intermediates.

We note that the use of DF/CD factorized integrals does not change the computational scaling of the DSRG-MRPT2 algorithm. However, there is a significant reduction in computational, memory, and I/O costs from avoiding the transformation of the four-index two-electron integrals necessary in a conventional implementation.[\[76\]](#)

### 3.4 Computational Details

In this work, we studied the singlet-triplet splittings ( $\Delta E_{\text{ST}} = E_{\text{S}} - E_{\text{T}}$ ) of ten naphthyne isomers. Each isomer is designated as  $(i, j)$ -naphthyne, and it is formally obtained by removing two hydrogens from the carbons at  $i$  and  $j$  positions of a naphthalene. Figure [3.4](#) shows the numbering scheme of naphthalene used in this work.

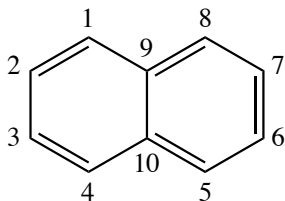


Figure 3.4: Naphthalene numbering scheme used in this study. The notation  $(i, j)$ -naphthyne indicates that two hydrogen atoms were removed from positions  $i$  and  $j$ .

Following Ref. [164](#), we optimized the geometry of singlet (1,3)-, (2,6)-, and (1,6)-naphthyne isomers at the CASSCF/cc-pVDZ level of theory with a CAS(4,4), CAS(2,2), and CAS(2,2) active space, respectively. All other naphthyne isomers were optimized using Becke’s three-parameter exchange[\[165\]](#) and Lee-Yang-Parr correlation[\[166\]](#) (B3LYP) functional and the cc-pVDZ[\[167\]](#) basis set. Unrestricted Kohn-Sham orbitals were used for both singlet and triplet states. Geometry optimizations were performed

using the NWChem [168] software package.

Table 3.3: Point group symmetries for all naphthyne isomers along with the corresponding minimal active spaces in Cotton’s ordering.[169] We use the following ordering for  $C_s$ ,  $C_{2v}$  and  $C_{2h}$ :  $(a', a'')$ ,  $(a_1, a_2, b_1, b_2)$ , and  $(a_g, b_g, a_u, b_u)$ . For example, the notation (2, 10) means that the active space is composed of two  $a'$  orbitals and ten  $a''$  orbitals. For (1,4)-, (1,8)-, (2,3)-, and (2,7)-naphthyne, the molecules are placed in the  $xz$  plane, where  $z$  is the  $C_2$  rotation axis. All other naphthyne are placed in the  $xy$  plane.

Isomer	Sym.	States	Active Space	
			CAS(2,2)	CAS(12,12)
1,2	$C_s$	$^1A'$ , $^3A'$	(2, 0)	(2, 10)
1,3	$C_s$	$^1A'$ , $^3A'$	(2, 0)	(2, 10)
1,4	$C_{2v}$	$^1A_1$ , $^3B_1$	(1, 0, 1, 0)	(1, 5, 1, 5)
1,5	$C_{2h}$	$^1A_g$ , $^3B_u$	(1, 0, 0, 1)	(1, 5, 5, 1)
1,6	$C_s$	$^1A'$ , $^3A'$	(2, 0)	(2, 10)
1,7	$C_s$	$^1A'$ , $^3A'$	(2, 0)	(2, 10)
1,8	$C_{2v}$	$^1A_1$ , $^3B_1$	(1, 0, 1, 0)	(1, 5, 1, 5)
2,3	$C_{2v}$	$^1A_1$ , $^3B_1$	(1, 0, 1, 0)	(1, 5, 1, 5)
2,6	$C_{2h}$	$^1A_g$ , $^3B_u$	(1, 0, 0, 1)	(1, 5, 5, 1)
2,7	$C_{2v}$	$^1A_1$ , $^3B_1$	(1, 0, 1, 0)	(1, 5, 1, 5)

State-specific DSRG-MRPT2 computations used a CASCI reference. The active spaces for different naphthyne isomers are reported in Table 3.3. Since at the moment we do not have access to a DF/CD CASSCF implementation, we opted for evaluating the energy of both the singlet and triplet states using restricted open-shell Hartree–Fock (ROHF) orbitals. This choice of orbitals is certainly not optimal, and may lead to an imbalanced treatment of singlet and triplet states. Dunning’s correlation-consistent cc-pVXZ ( $X = D, T, Q, 5$ ) basis sets[167, 170] were used to deduce basis set effects, and the corresponding auxiliary basis sets were chosen as cc-pVXZ-JKFIT basis sets[171] for ROHF computations and cc-pVXZ-RI basis sets[159, 172] for DSRG-MRPT2 computations. We used a value of  $s = 0.5 E_h^{-2}$ , and kept the 1s-like orbitals on carbon atoms frozen for all DSRG-MRPT2 computations.

## 3.5 Results

### 3.5.1 Singlet-triplet splittings of naphthylene diradicals

In this section we will demonstrate how our efficient implementation of the DSRG-MRPT2 can be used to obtain the singlet-triplet splitting of naphthylenes with fairly large basis sets. Among arynes,[173–175] the electronic structure of *ortho*, *meta*, and *para* benzyne has been well characterized from the point of view of both experiment and theory.[164, 176–182] However, in the case of naphthylenes, singlet-triplet splittings have been investigated mostly by theoretical studies[164, 177, 183, 184] and, to the best of our knowledge, no experimental values have been reported.

Table 3.4: Analysis of the DSRG-MRPT2 energy error (in kcal mol<sup>-1</sup>) introduced by density fitting (DF) and Cholesky decomposition (CD). Statistics were computed from the singlet-triplet splittings of the ten naphthylene isomers. Density fitting results were obtained using the cc-pVDZ-RI auxiliary basis set, while Cholesky vectors were generated using a threshold of 10<sup>-5</sup>  $E_h$ .

Factorization	Statistics	VDZ* <sup>a</sup>	cc-pVDZ
DF	MAX <sup>b</sup>	0.017	0.017
	MAE <sup>c</sup>	0.007	0.007
	$\sigma^d$	0.005	0.005
CD	MAX <sup>b</sup>	0.003	0.004
	MAE <sup>c</sup>	0.002	0.002
	$\sigma^d$	0.001	0.001

<sup>a</sup> The VDZ\* basis set is constructed from the cc-pVDZ basis set by removing the  $p$  functions for hydrogen atoms.

<sup>b</sup> Maximum absolute error:  $\text{MAX} = \max(|\Delta_i|)$ .

<sup>c</sup> Mean absolute error:  $\text{MAE} = \frac{1}{10} \sum_{i=1}^{10} |\Delta_i|$ .

<sup>d</sup> Standard deviation:  $\sigma = [\frac{1}{10} \sum_{i=1}^{10} (\Delta_i - \bar{\Delta})^2]^{1/2}$ , where  $\bar{\Delta} = \frac{1}{10} \sum_{i=1}^{10} \Delta_i$ .

We first verify the accuracy of the integral factorization techniques by performing DSRG-MRPT2 computations with DF, CD, and conventional integrals. Table 3.4 reports an analysis of the errors introduced by the DF and CD approximations when applied to compute  $\Delta_{\text{ST}}$ . These results show that both approximations introduce errors that are well within chemical accuracy: the maximum absolute error for DF and CD is only 0.017 and 0.003 kcal mol<sup>-1</sup>, respectively.

Table 3.5: Adiabatic singlet-triplet splittings ( $\Delta E_{ST} = E_S - E_T$ ) of naphthyne diradicals computed with the DF-DSRG-MRPT2 approach and a variety of basis sets. All computations utilized ROHF triplet orbitals. Carbon 1s-like orbitals were excluded from the DSRG-MRPT2 treatment of correlation energy.

		Naphthyne Isomers									
Active Space	Basis	Group I		Group II			Group III				
		1,2	2,3	1,3	1,5	1,6	1,4	2,7	2,6	1,7	1,8
CAS(2,2)	cc-pVDZ	-30.2	-24.9	-11.7	1.3	1.4	6.4	0.9	1.3	5.2	3.7
	cc-pVTZ	-33.5	-28.3	-14.1	0.3	-0.8	5.3	0.3	-0.8	4.2	3.0
	cc-pVQZ	-34.4	-29.2	-14.4	0.0	-1.1	5.1	0.1	-1.1	4.1	2.9
	cc-pV5Z	-34.7	-29.5	-14.5	0.0	-1.2	5.1	0.0	-1.1	4.0	2.9
CAS(12,12)	cc-pVDZ	-29.0	-24.3	-11.0	0.8	2.0	5.3	1.3	1.3	5.2	4.3
	cc-pVTZ	-32.6	-27.8	-13.7	-0.4	-0.2	4.2	0.6	-0.8	4.2	3.4
	cc-pVQZ	-33.6	-28.9	-14.2	-0.6	-0.5	4.1	0.3	-1.0	4.0	3.3
$c_1/c_2^a$		2.6	2.5	1.6	1.3	1.0	1.3	1.1	1.0	1.1	1.2

<sup>a</sup> The ratio of CI coefficients between the two dominant determinants in a CAS(2,2). This characteristic was used to separate the naphthynes into three separate groups.

Table 3.5 reports adiabatic singlet-triplet splittings of the ten naphthyne isomers computed with the DSRG-MRPT2 approach using various basis sets (cc-pVXZ, with  $X = D, T, Q, 5$ ). These results were computed using two active spaces: 1) CAS(2,2) which consists of two carbon  $\sigma$  orbitals on radical centers and 2) CAS(12,12), which augments the CAS(2,2) space with ten carbon  $\pi$  orbitals.

Following the analysis of Squires and Cramer,[177] we separate the naphthyne isomers into three different groups characterized by different magnitudes of the singlet-triplet splitting.[164] Group I naphthyne, which consists of (1,2) and (2,3)-naphthyne, have adjacent radical centers and their  $\Delta_{ST}$  is comparable to that of *o*-benzyne ( $-37.5 \pm 0.3$  kcal mol<sup>-1</sup>, from experiment).[178] For group I naphthyne, through-bond interactions[176, 177] tend to stabilize the singlet state and are thus responsible for the relatively large  $\Delta_{ST}$  value. Our best DSRG-MRPT2 estimates for the  $\Delta E_{ST}$  of (1,2) and (2,3)-naphthyne are  $-33.6$  and  $-28.9$  kcal mol<sup>-1</sup>, respectively.

Group II contains (1,3)-naphthyne, the only isomer with the two radical centers in *meta* position. Our best estimate for the  $\Delta_{ST}$  value of this isomer is  $-14.2$  kcal mol<sup>-1</sup>, which is comparable to the value for *m*-benzyne ( $-21.0$  kcal mol<sup>-1</sup>). Going from group I to II, there is a buildup of diradical character, which is reflected in the ratio between the two dominant configurations of the CAS(2,2) reference. This quantity is reported at the bottom of Table 3.5, and it goes from 2.6–2.5 for group I to 1.6 for group II naphthyne. Group III naphthyne have singlet-triplet splittings that range from  $-1.0$  to  $+4.1$  kcal mol<sup>-1</sup>. This range is comparable to the  $\Delta_{ST}$  of *p*-benzyne ( $-3.8$  kcal mol<sup>-1</sup>). As indicated by the small  $c_1/c_2$  ratio, these species are almost pure diradicals.

Table 3.6: Adiabatic singlet-triplet splittings ( $\Delta E_{ST} = E_S - E_T$ ) of naphthyne diradicals computed with the DSRG-MRPT2, CASPT2, and RMR-CCSD(T) approaches. All DSRG-MRPT2 computations used triplet ROHF orbitals and the cc-pVDZ-RI auxiliary basis set. RMR-CCSD(T) results used RHF and ROHF orbitals for singlet and triplet states, respectively. CASPT2 results used CASSCF(12,12) orbitals. RMR-CCSD(T) and DSRG-MRPT2 results are based on the same geometries (from DFT and CASSCF, see Sec. 3.4), while CASPT2 results are based on CASSCF(12,12) optimized geometries. The VDZ\* basis set is constructed from the cc-pVDZ basis set by removing hydrogen  $p$  functions.

		Naphthyne Isomers									
CAS/Basis	Method	Group I		Group II	Group III						
		1,2	2,3	1,3	1,5	1,6	1,4	2,7	2,6	1,7	1,8
(2,2)/VDZ*	RMR-CCSD(T) <sup>a</sup>	-35.2	-28.9	-12.7	-0.3	2.1	1.6	2.9	5.7	6.5	6.5
	DSRG-MRPT2 <sup>b</sup>	-30.2	-25.0	-11.6	1.3	1.5	6.4	0.8	1.5	5.2	3.8
	CASPT2 <sup>c</sup>	-31.8	-27.7	-17.5	-8.6	-2.2	-6.7	-3.9	-3.0	-2.7	-1.8
(12,12)/cc-pVDZ	DSRG-MRPT2 <sup>b</sup>	-31.3	-27.5	-14.7	-3.1	2.3	0.9		1.6	4.1	3.1
	DSRG-MRPT2 <sup>b</sup>	-29.0	-24.3	-11.0	0.8	2.0	5.3		1.6	4.1	3.1

<sup>a</sup> From Ref. 164.

<sup>b</sup> This work.

<sup>c</sup> From Ref. 177.

Table 3.6 reports a comparison between our CAS(2,2) DSRG-MRPT2 results and the reduced multireference coupled cluster with singles, doubles, and perturbative triples [RMR-CCSD(T)] results of Li and Paldus[164] using the same geometries and basis set. Our DSRG-MRPT2 results for group I and II isomers agree very well with those from RMR-CCSD(T): the maximum deviations are respectively 3.8 and 1.1 kcal mol<sup>-1</sup>. In the case of group III naphthynes, the disagreement between the DSRG-MRPT2 and RMR-CCSD(T) results is slightly less favorable. The assignment of the ground state is consistent among the two methods, except for the (1,5) isomer, and (1,4)-naphthyne displays the largest absolute error (4.8 kcal mol<sup>-1</sup>).

Table 3.6 also reports a comparison between our DSRG-MRPT2 results and the CASPT2 results of Squires and Cramer,[177] both obtained using a CAS(12,12) reference. Note, that the comparison of these two sets of computations is complicated by the fact that the naphthynes geometries and orbitals used in these studies are different: the CASPT2 calculations use CASSCF(12,12) optimized geometries and orbitals. As a consequence, the DSRG-MRPT2 results show some significant disagreements with the CASPT2 results. For example, the DSRG-MRPT2 results favor triplet ground states for all the group III isomers, while CASPT2 predicts exactly the opposite. Notice that the RMR-CCSD(T) approach also predicts triplet ground states for all group III naphthynes, except for the (1,5) isomer.

To illustrate the importance of the geometry used to compute  $\Delta_{ST}$ , we optimized the singlet and triplet state geometry of (1,4)-naphthyne with the Mukherjee multireference coupled cluster approach with singles and doubles (Mk-MRCCSD) using the cc-pVDZ basis set and a CASSCF(2,2) reference. At this level of theory, the singlet state is predicted to be the ground state and the adiabatic  $\Delta_{ST} = -4.98$  kcal mol<sup>-1</sup>. The Mk-MRCCSD  $\Delta_{ST}$  of (1,4)-naphthyne agrees well with the experimental  $\Delta_{ST}$  of *p*-benzyne, indicating that the nature of these two diradicals is similar. More importantly, this result is also in agreement with the ground state assignment of CASPT2

computations.[177] DSRG-MRPT2  $\Delta_{\text{ST}}$  computed using the Mk-MRCCSD/cc-pVDZ geometries also favor a singlet ground state. For example, when using ROHF orbitals, the DSRG-MRPT2  $\Delta_{\text{ST}}$  is equal to  $-0.9 \text{ kcal mol}^{-1}$  [CAS(2,2)] and  $-1.98 \text{ kcal mol}^{-1}$  [CAS(12,12)]. The use of CASSCF orbitals improves the agreement with the Mk-MRCCSD data: the corresponding  $\Delta_{\text{ST}}$  are  $-2.27 \text{ kcal mol}^{-1}$  [CAS(2,2)] and  $-3.82 \text{ kcal mol}^{-1}$  [CAS(12,12)]. As anticipated, ROHF orbitals tend to favor the triplet state, shifting  $\Delta_{\text{ST}}$  by  $\sim 1.5 \text{ kcal mol}^{-1}$ . Although these results are not conclusive, they do suggest that to obtain reliable estimates of  $\Delta_{\text{ST}}$  for the naphthyne is it necessary to employ geometries optimized at a high level of theory.

In addition to adiabatic singlet-triplet splittings, in Table 3.7 we report a comparison of the vertical DSRG-MRPT2 splittings with those from highly-accurate multireference coupled cluster (MRCC) computations by Brabec and coworkers.[183] These authors reported  $\Delta_{\text{ST}}$  for (2,7)-, (2,6)-, (1,7)- and (1,8)-naphthyne computed with the Brillouin–Wigner (BW) MRCC approach with the *a posteriori* correction[104, 185] and the Mk-MRCCSD approach. To facilitate this comparison, all DSRG-MRPT2 results in Table 3.7 are computed using the same type of orbitals (restricted Hartree–Fock) and geometries used by Brabec et al.[183] The DSRG-MRPT2 results agree well with those from BW-MRCCSD: both methods agree in the assignment of the

Table 3.7: A comparison of the vertical singlet-triplet splitting between MRCC and the DSRG-MRPT2. All of these results use singlet geometries, RHF orbitals, and a CAS(2,2).

Method	Basis	Naphthyne Isomers			
		2,7	2,6	1,7	1,8
DSRG-MRPT2 <sup>a</sup>	cc-pVDZ	-3.0	0.2	-1.6	-2.6
	cc-pVTZ	-3.2	0.2	-1.7	-2.8
BW-MRCCSD <sup>b</sup>	cc-pVDZ	-0.46	1.39	-0.34	-1.40
	cc-pVTZ	-0.78	1.05	-0.50	-1.47
Mk-MRCCSD <sup>b</sup>	cc-pVDZ	6.47	8.48	7.29	3.82
	cc-pVTZ	7.16	9.79	6.79	4.43

<sup>a</sup> This work.

<sup>b</sup> From Ref. 184

ground state and the maximum error is only 2.54 kcal mol<sup>-1</sup>. Note, that there is a substantial disagreement between the BW- and Mk-MRCCSD results, which was attributed to the *a posteriori* corrections used in BW-MRCCSD.[184]

### 3.5.2 Scaling with respect to basis set and active space size

In this section we illustrate the efficiency of our DSRG-MRPT2 by reporting timings for the single-point energy computation of singlet (2,3)-naphthylene. DSRG-MRPT2 timings for basis sets that range from 152 to 1240 orbitals are reported in Table 3.8. Due to the efficiency of the DF approximation, DSRG-MRPT2 computations with 1000–1500 may be performed routinely. Indeed, our largest calculation using a CAS(2,2) reference and the cc-pV5Z basis set takes about 5 minutes with 8 threads on an Intel Xeon E5-2650 v2 processor. This time is only about 5% of the total time required (110 minutes), with the majority of the remaining part of the computation spent building the Fock matrix (20 minutes) and the generation of the MO transformed DF integrals (35 minutes). The timings for the CAS(2,2) computations as function of the basis set size nicely follow the quadratic scaling expected from the DSRG-MRPT2 equations when the number of core and active orbitals is kept fixed. Going from the CAS(2,2) to the CAS(12,12) active space we notice an increase of a factor 3–4 of the timing for the DSRG-MRPT2 step. This result is significant because it suggests that for the active space here considered, terms that scale as a power of the number of active orbitals have a very small prefactor. Indeed, even with the CAS(12,12) reference, the most expensive steps in the energy computation are the generation of the amplitudes  $t_{ij}^{ab}$  and  $\tilde{v}_{ef}^{mn}$ , which require respectively 52% and 27% of the total time.

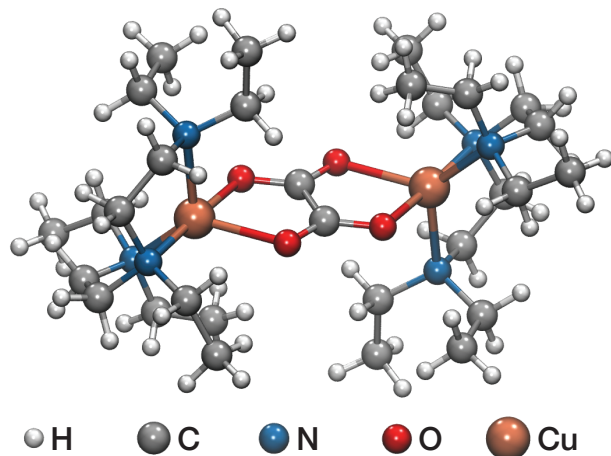


Figure 3.5: Example of a transition metal complex,  $[(\text{Et}_5\text{dien})_2\text{Cu}_2^{\text{II}}(\mu\text{-C}_2\text{O}_4)]^{2+}$ , that can be treated with the DF-DSRG-MRPT2 approach. Singlet state computed with a CAS(2,2) active space, ROHF triplet orbitals, and the def2-TZVP basis set (1726 basis functions). The DF-DSRG-MRPT2 computation ran in about 5.2 hours on a Intel Xeon E5-2650 v2 processor using 8 threads. Geometry taken from Ref. 186.

Table 3.8: Timing of DSRG-MRPT2 naphthynes computations ( $T_{\text{PT2}}$ , in seconds) as a function of basis set size ( $N$ ). The total time ( $T$ ) includes the CASCI step, generation of the DF integrals, and evaluation of the DSRG-MRPT2 energy. These computations ran on one Intel Xeon E5-2650 v2 processor using 8 threads.

Active Space	Basis	$N$	$T_{\text{PT2}}$	$T_{\text{PT2}}/T$ %
CAS(2,2)	cc-pVDZ	170	3.5	21.0
	cc-pVTZ	384	22.6	18.6
	cc-pVQZ	730	93.6	7.8
	cc-pV5Z	1240	316.5	4.8
CAS(12,12)	cc-pVDZ	170	13.2	9.6
	cc-pVTZ	384	72.1	27.8
	cc-pVQZ	730	284.3	26.5

In addition to computations on the naphthynes, in Fig. 3.5 we show an example of a large transition metal complex (108 atoms) taken from the work of Mayhall and Head-Gordon[186] that can be studied in a reasonable amount of time with our DF-DSRG-MRPT2 implementation. The DF-DSRG-MRPT2 correlation energy of the open-shell singlet state of this complex was computed using a CAS(2,2) active space and a def2-TZVP basis set[187] (1726 basis functions) in about 5.2 hours on one Intel Xeon E5-2650 v2 processor using 8 threads. This examples shows that our

DF-DSRG-MRPT2 implementation can be routinely applied to systems with 50–100 atoms using a triple- $\zeta$  quality basis set.

## 3.6 Conclusion

In this work, we presented a new formulation of the DSRG-MRPT2 approach that takes advantage of two-electron integral factorization and the structure of CAS density matrices. We propose an algorithm that is similar to the one used to evaluate the DF-MP2 energy. This algorithm has reduced memory requirements and allows the routine application of the DSRG-MRPT2 to systems with up to 100 atoms (1500–2000 basis functions).

To demonstrate the applicability of this novel DSRG-MRPT2 implementation to medium-sized system we studied the singlet-triplet splittings for the ten isomers of naphthylene diradicals. We reported computations with CAS(2,2) and CAS(12,12) active spaces and up to quintuple- $\zeta$  quality basis sets (1240 basis functions). Overall, the DSRG-MRPT2 results are in good agreement with previously reported adiabatic singlet-triplet splittings computed at the RMR-CCSD(T)/VDZ\* level of theory: the mean absolute deviation between the two approaches is only 2.7 kcal mol<sup>-1</sup>. We find that the singlet-triplet splittings of Group III naphthylenes are strongly dependent on the quality of the molecular geometries. This fact makes the comparison with previously reported CASPT2 results more difficult to analyze. It also suggests that extra caution is required to interpret highly-correlated results for naphthylenes based on DFT or CASSCF geometries. DSRG-MRPT2 computations with larger bases suggest that one should at least use a triple- $\zeta$  basis set to converge the singlet-triplet splitting of Group III naphthylenes to 0.4 kcal mol<sup>-1</sup>, while a quadruple- $\zeta$  basis is necessary to reduce this error to about 0.1 kcal mol<sup>-1</sup>.

In this work we have showed that the cost of evaluating the DSRG-MRPT2 energy can be significantly reduced by resorting to integral factorization techniques. Nev-

ertheless, the computational scaling of integral-factorized DSRG-MRPT2 remains proportional to the fifth power of the number of electrons. Therefore, to apply this approach to systems with 100–150 atoms it will be necessary to reduce its computational scaling. Given the simplicity of the DSRG-MRPT2 equations, an interesting option is to combine the prescreening of atomic orbital (AO) integrals with Laplace transformation of the energy denominators.[77, 79, 188–190] One novel issue that arises in the application of the Laplace transformation to the DSRG-MRPT2 approach is the fact that the energy denominators are renormalized. However, we think that this problem may be addressed either by finding a suitable decomposition of the renormalized denominators, or by redefining the source operator to treat the most expensive contributions (from diagram F1–F3) as non-renormalized quantities. We anticipate that the Laplace-transformed AO-DSRG-MRPT2 will be an essential tool to go beyond the current limit of 2000 basis functions.

## Bibliography

- [1] Aron J Cohen, Paula Mori-Sánchez, and Weitao Yang. Insights into current limitations of density functional theory. *Science*, 321(5890):792–4, Aug 2008.
- [2] Axel D Becke. Perspective: Fifty years of density-functional theory in chemical physics. *J Chem Phys*, 140(18):18A301, May 2014.
- [3] A. Dreuw and M. Head-Gordon. Failure of time-dependent density functional theory for long-range charge-transfer excited states: The zincbacteriochlorin-bacteriochlorin and bacteriochlorophyll-spheroidene complexes. *J. Am. Chem. Soc.*, 126(12):4007–4016, March 2004. ISSN 0002-7863. doi: 10.1021/ja039556n.
- [4] Peter Elliott, Sharma Goldson, Chris Canahui, and Neepa T Maitra. Perspectives on double-excitations in tddft. *Chemical Physics*, 391(1):110–119, 2011.
- [5] Paolo Celani and Hans-Joachim Werner. Multireference perturbation theory for large restricted and selected active space reference wave functions. *The Journal of Chemical Physics*, 112(13):5546–5557, 2000.
- [6] Michael W Schmidt and Mark S Gordon. The construction and interpretation of mscf wavefunctions. *Annu. Rev. Phys. Chem.*, 49(1):233–266, 1998.
- [7] Isaiah Shavitt and Rodney J Bartlett. *Many-body methods in chemistry and physics: MBPT and coupled-cluster theory*. Cambridge molecular science. Cambridge University Press, Cambridge, 2009. ISBN 9780521818322.
- [8] Attila Szabo and Neil S Ostlund. *Modern quantum chemistry: introduction to advanced electronic structure theory*. Dover Publications, Mineola, N.Y., 1996. ISBN 0486691861 (pbk.).

- [9] Jan Almlöf, K Faegri, and Knut Korsell. Principles for a direct scf approach to licao–moab-initio calculations. *J. Comp. Chem.*, 3(3):385–399, 1982.
- [10] Marco Häser and Jan Almlöf. Laplace transform techniques in mo/ller–plesset perturbation theory. *The Journal of chemical physics*, 96(1):489–494, 1992.
- [11] Ananth Grama. *Introduction to parallel computing*. Pearson Education, 2003.
- [12] Curtis L Janssen and Ida MB Nielsen. *Parallel computing in quantum chemistry*. CRC Press, 2008.
- [13] Marco Häser and Reinhart Ahlrichs. Improvements on the direct scf method. *J. Comp. Chem.*, 10(1):104–111, 1989.
- [14] Takeshi Yanai and Garnet Kin-Lic Chan. Canonical transformation theory for multireference problems. *The Journal of chemical physics*, 124(19):194106, 2006.
- [15] Kevin P Hannon, Chenyang Li, and Francesco A Evangelista. An integral-factorized implementation of the driven similarity renormalization group second-order multireference perturbation theory. *The Journal of Chemical Physics*, 144(20):204111, 2016.
- [16] Trygve Helgaker, Poul Jorgensen, and Jeppe Olsen. *Molecular Electronic-Structure Theory*. Wiley, 2013.
- [17] Carmen J Calzado, Jesús Cabrero, Jean Paul Malrieu, and Rosa Caballol. Analysis of the magnetic coupling in binuclear complexes. i. physics of the coupling. *J. Chem. Phys.*, 116(7):2728–2747, 2002.
- [18] Carmen J Calzado, Jesús Cabrero, Jean Paul Malrieu, and Rosa Caballol. Analysis of the magnetic coupling in binuclear complexes. ii. derivation of valence

- effective hamiltonians from ab initio ci and dft calculations. *J. Chem. Phys.*, 116(10):3985–4000, 2002.
- [19] Carmen J Calzado, Celestino Angeli, David Taratiel, Rosa Caballol, and Jean-Paul Malrieu. Analysis of the magnetic coupling in binuclear systems. iii. the role of the ligand to metal charge transfer excitations revisited. *J. Chem. Phys.*, 131(4):044327, 2009.
- [20] Jean Paul Malrieu, Rosa Caballol, Carmen J Calzado, Coen De Graaf, and Nathalie Guihery. Magnetic interactions in molecules and highly correlated materials: physical content, analytical derivation, and rigorous extraction of magnetic hamiltonians. *Chem. Rev.*, 114(1):429–492, 2013.
- [21] Leticia González, Daniel Escudero, and Luis Serrano-Andrés. Progress and challenges in the calculation of electronic excited states. *Chem. Phys. Chem.*, 13(1):28–51, 2012.
- [22] A. Dreuw and M. Head-Gordon. Single-reference ab initio methods for the calculation of excited states of large molecules. *Chem. Rev.*, 105(11):4009–4037, November 2005. ISSN 0009-2665. doi: 10.1021/cr0505627.
- [23] Marko Schreiber, Mario R Silva-Junior, Stephan PA Sauer, and Walter Thiel. Benchmarks for electronically excited states: Caspt2, cc2, ccsd, and cc3. *J. Chem. Phys.*, 128(13):134110, 2008.
- [24] Björn O Roos, Peter R Taylor, and P. E. M. SIEGBAHN. A complete active space scf method (casscf) using a density matrix formulated super-ci approach. *Chem. Phys.*, 48(2):157–173, 1980.
- [25] Jeppe Olsen. The casscf method: A perspective and commentary. *Int. J. Quant. Chem.*, 111(13):3267–3272, 2011.

- [26] P. E. M. Siegbahn, J Almlöf, A. Heiberg, and B. O. Roos. The complete active space scf (casscf) method in a newton-raphson formulation with application to the hno molecule. *J. Chem. Phys.*, 74(4):2384–2396, 1981. ISSN 0021-9606.
- [27] Péter G Szalay, Thomas Mueller, Gergely Gidofalvi, Hans Lischka, and Ron Shepard. Multiconfiguration self-consistent field and multireference configuration interaction methods and applications. *Chem. Rev.*, 112(1):108–181, 2011.
- [28] Jacob Fosso-Tande, Truong-Son Nguyen, Gergely Gidofalvi, and A Eugene De-Prince. Large-scale v2rdm-driven casscf methods. *J. Chem. Theory Comput.*, 12:2260, 2016.
- [29] Byron H Lengsfeld III. General second order mcscf theory: a density matrix directed algorithm. *J. Chem. Phys.*, 73(1):382–390, 1980.
- [30] Hans-Joachim Werner and Wilfried Meyer. A quadratically convergent mcscf method for the simultaneous optimization of several states. *J. Chem. Phys.*, 74(10):5794–5801, 1981.
- [31] Hans-Joachim Werner and Peter J Knowles. A second order multiconfiguration scf procedure with optimum convergence. *J. Chem. Phys.*, 82(11):5053–5063, 1985.
- [32] Francesco Aquilante, Thomas Bondo Pedersen, Roland Lindh, Björn Olof Roos, Alfredo Sánchez de Merás, and Henrik Koch. Accurate ab initio density fitting for multiconfigurational self-consistent field methods. *J. Chem. Phys.*, 129(2):024113, 2008.
- [33] James W Snyder Jr, Edward G Hohenstein, Nathan Luehr, and Todd J Martínez. An atomic orbital-based formulation of analytical gradients and nonadiabatic coupling vector elements for the state-averaged complete active space

- self-consistent field method on graphical processing units. *J. Chem. Phys.*, 143(15):154107, 2015.
- [34] Edward G Hohenstein, Nathan Luehr, Ivan S Ufimtsev, and Todd J Martínez. An atomic orbital-based formulation of the complete active space self-consistent field method on graphical processing units. *J. Chem. Phys.*, 142(22):224103, 2015.
- [35] GD Fletcher. A parallel multi-configuration self-consistent field algorithm. *Mol. Phys.*, 105(23-24):2971–2976, 2007.
- [36] Francesco Aquilante, Per-Åke Malmqvist, Thomas Bondo Pedersen, Abhik Ghosh, and Björn Olof Roos. Cholesky decomposition-based multiconfiguration second-order perturbation theory (cd-caspt2): Application to the spin-state energetics of coiii (diiminato)(nph). *J. Chem. Theory Comput.*, 4(5):694–702, 2008.
- [37] Henrik Koch, Alfredo Sánchez de Merás, and Thomas Bondo Pedersen. Reduced scaling in electronic structure calculations using cholesky decompositions. *J. Chem. Phys.*, 118(21):9481–9484, 2003.
- [38] Francesco Aquilante, Linus Boman, Jonas Boström, Henrik Koch, Roland Lindh, Alfredo Sánchez de Merás, and Thomas Bondo Pedersen. Cholesky decomposition techniques in electronic structure theory. In *Linear-Scaling Techniques in Computational Chemistry and Physics*, pages 301–343. Springer, 2011.
- [39] Nelson HF Beebe and Jan Linderberg. Simplifications in the generation and transformation of two-electron integrals in molecular calculations. *Int. J. Quant. Chem.*, 12(4):683–705, 1977.
- [40] Brett I Dunlap, JWD Connolly, and JR Sabin. On some approximations in applications of  $x\alpha$  theory. *J. Chem. Phys.*, 71(8):3396–3402, 1979.

- [41] Rick A Kendall and Herbert A Früchtl. The impact of the resolution of the identity approximate integral method on modern ab initio algorithm development. *Theor. Chem. Acc.*, 97(1-4):158–163, 1997.
- [42] Christoph Köppl and Hans-Joachim Werner. Parallel and low-order scaling implementation of hartree-fock exchange using local density fitting. *J. Chem. Theory Comput.*, 12(7):3122–34, Jul 2016. doi: 10.1021/acs.jctc.6b00251.
- [43] Wibe A de Jong, Eric Bylaska, Niranjan Govind, Curtis L Janssen, Karol Kowalski, Thomas Müller, Ida MB Nielsen, Hubertus JJ van Dam, Valera Veryazov, and Roland Lindh. Utilizing high performance computing for chemistry: parallel computational chemistry. *Phys. Chem. Chem. Phys.*, 12(26):6896–6920, 2010.
- [44] Ivan S Ufimtsev and Todd J Martinez. Quantum chemistry on graphical processing units. 1. strategies for two-electron integral evaluation. *J. Chem. Theory Comput.*, 4(2):222–231, 2008.
- [45] Andrey Asadchev and Mark S Gordon. New multithreaded hybrid cpu/gpu approach to hartree-fock. *J. Chem. Theory Comput.*, 8(11):4166–4176, 2012.
- [46] Leslie Vogt, Roberto Olivares-Amaya, Sean Kermes, Yihan Shao, Carlos Amador-Bedolla, and Alán Aspuru-Guzik. Accelerating resolution-of-the-identity second-order møller-plesset quantum chemistry calculations with graphical processing units. *J. Phys. Chem. A*, 112(10):2049–2057, 2008.
- [47] Edoardo Aprà and Karol Kowalski. Implementation of high-order multireference coupled-cluster methods on intel many integrated core architecture. *J. Chem. Theory Comput.*, 12(3):1129–1138, 2016.
- [48] September 2016. URL <https://www.top500.org/lists/2016/06/>.

- [49] Edmond Chow, Xing Liu, Mikhail Smelyanskiy, and Jeff R Hammond. Parallel scalability of hartree–fock calculations. *J. Chem. Phys.*, 142(10):104103, 2015.
- [50] Edmond Chow, Xing Liu, Sanchit Misra, Marat Dukhan, Mikhail Smelyanskiy, Jeff R Hammond, Yunfei Du, Xiang-Ke Liao, and Pradeep Dubey. Scaling up hartree–fock calculations on tianhe-2. *International Journal of High Performance Computing Applications*, page 1094342015592960, 2015.
- [51] Xing Liu, Aftab Patel, and Edmond Chow. A new scalable parallel algorithm for fock matrix construction. In *Parallel and Distributed Processing Symposium, 2014 IEEE 28th International*, pages 902–914. IEEE, 2014.
- [52] Galina Chaban, Michael W Schmidt, and Mark S Gordon. Approximate second order method for orbital optimization of scf and mscf wavefunctions. *Theor. Chem. Acc.*, 97(1-4):88–95, 1997.
- [53] B Scott Fales and Benjamin G Levine. Nanoscale multireference quantum chemistry: Full configuration interaction on graphical processing units. *J. Chem. Theory Comput.*, 11(10):4708–4716, 2015.
- [54] Sebastian Wouters and Dimitri Van Neck. The density matrix renormalization group for ab initio quantum chemistry. *Eur. Phys. J. D*, 68(9):1–20, 2014.
- [55] Garnet Kin-Lic Chan and Martin Head-Gordon. Highly correlated calculations with a polynomial cost algorithm: A study of the density matrix renormalization group. *J. Chem. Phys.*, 116(11):4462–4476, 2002.
- [56] Takeshi Yanai, Yuki Kurashige, Debashree Ghosh, and Garnet Kin Chan. Accelerating convergence in iterative solution for large-scale complete active space self-consistent-field calculations. *Int. J. Quant. Chem.*, 109(10):2178–2190, 2009.

- [57] Garnet Kin-Lic Chan, Sandeep Sharma, S. R. Leone, P. S. Cremer, J. T. Groves, and M. A. Johnson. The density matrix renormalization group in quantum chemistry. *Annu. Rev. Phys. Chem.*, 62:465–481, 2011. ISSN 0066-426X. doi: 10.1146/annurev-physchem-032210-103338.
- [58] Roberto Olivares-Amaya, Weifeng Hu, Naoki Nakatani, Sandeep Sharma, Jun Yang, and Garnet Kin-Lic Chan. The ab-initio density matrix renormalization group in practice. *J. Chem. Phys.*, 142(3):034102, 2015.
- [59] Giovanni Li Manni, Simon D Smart, and Ali Alavi. Combining the complete active space self-consistent field method and the full configuration interaction quantum monte carlo within a super-ci framework, with application to challenging metal-porphyrins. *J. Chem. Theory Comput.*, 12(3):1245–1258, 2016.
- [60] Robert E Thomas, Qiming Sun, Ali Alavi, and George H Booth. Stochastic multiconfigurational self-consistent field theory. *J. Chem. Theory Comput.*, 11(11):5316–5325, 2015.
- [61] Justin M Turney, Andrew C Simmonett, Robert M Parrish, Edward G Hohenstein, Francesco A Evangelista, Justin T Fermann, Benjamin J Mintz, Lori A Burns, Jeremiah J Wilke, Micah L Abrams, et al. Psi4: an open-source ab initio electronic structure program. *Wiley Interdisciplinary Reviews: Computational Molecular Science*, 2(4):556–565, 2012.
- [62] Thom H Dunning Jr. Gaussian basis sets for use in correlated molecular calculations. i. the atoms boron through neon and hydrogen. *J. Chem. Phys.*, 90(2):1007–1023, 1989.
- [63] Nicholas J Mayhall and Martin Head-Gordon. Increasing spin-flips and decreasing cost: Perturbative corrections for external singles to the complete active

- space spin flip model for low-lying excited states and strong correlation. *J. Chem. Phys.*, 141(4):044112, 2014.
- [64] Florian Weigend and Reinhart Ahlrichs. Balanced basis sets of split valence, triple zeta valence and quadruple zeta valence quality for h to rn: design and assessment of accuracy. *Phys. Chem. Chem. Phys.*, 7(18):3297–3305, 2005.
- [65] Gene H Golub and Charles F Van Loan. *Matrix Computations*. Johns Hopkins University Press, 2012.
- [66] Cleve Moler and Charles Van Loan. Nineteen dubious ways to compute the exponential of a matrix, twenty-five years later. *SIAM Rev.*, 45(1):3–49, 2003.
- [67] So Hirata, Xiao He, Matthew R Hermes, and Soohaeng Y Willow. Second-Order Many-Body Perturbation Theory: An Eternal Frontier. *J. Phys. Chem. A*, 118(4):655–672, January 2014.
- [68] Jerry L Whitten. Coulombic potential energy integrals and approximations. *J. Chem. Phys.*, 58(10):4496–4501, 1973.
- [69] Brett I Dunlap, JWD Connolly, and JR Sabin. On some approximations in applications of  $x\alpha$  theory. *J. Chem. Phys.*, 71(8):3396–3402, 1979.
- [70] Nelson HF Beebe and Jan Linderberg. Simplifications in the generation and transformation of two-electron integrals in molecular calculations. *Int. J. Quantum Chem.*, 12(4):683–705, 1977.
- [71] Henrik Koch, Alfredo Sánchez de Merás, and Thomas Bondo Pedersen. Reduced scaling in electronic structure calculations using cholesky decompositions. *J. Chem. Phys.*, 118(21):9481–9484, 2003.
- [72] Francesco Aquilante, Thomas Bondo Pedersen, and Roland Lindh. Low-cost evaluation of the exchange fock matrix from cholesky and density fitting repre-

- sentations of the electron repulsion integrals. *J. Chem. Phys.*, 126(19):194106, 2007. doi: <http://dx.doi.org/10.1063/1.2736701>. URL <http://scitation.aip.org/content/aip/journal/jcp/126/19/10.1063/1.2736701>.
- [73] Francesco Aquilante, Laura Gagliardi, Thomas Bondo Pedersen, and Roland Lindh. Atomic cholesky decompositions: A route to unbiased auxiliary basis sets for density fitting approximation with tunable accuracy and efficiency. *J. Chem. Phys.*, 130(15):154107, 2009. doi: <http://dx.doi.org/10.1063/1.3116784>. URL <http://scitation.aip.org/content/aip/journal/jcp/130/15/10.1063/1.3116784>.
- [74] Francesco Aquilante, Linus Boman, Jonas Boström, Henrik Koch, Roland Lindh, Alfredo Sánchez de Merás, and Thomas Bondo Pedersen. Cholesky decomposition techniques in electronic structure theory. In Robert Zalesny, Manthos G. Papadopoulos, Paul G. Mezey, and Jerzy Leszczynski, editors, *Linear-Scaling Techniques in Computational Chemistry and Physics*, volume 13 of *Challenges and Advances in Computational Chemistry and Physics*, pages 301–343. Springer Netherlands, 2011. ISBN 978-90-481-2852-5. doi: [10.1007/978-90-481-2853-2\\_13](https://doi.org/10.1007/978-90-481-2853-2_13). URL [http://dx.doi.org/10.1007/978-90-481-2853-2\\_13](http://dx.doi.org/10.1007/978-90-481-2853-2_13).
- [75] Nicholas J Higham. Cholesky factorization. *WIREs: Comp. Stat.*, 1(2):251–254, September 2009.
- [76] Hans-Joachim Werner, Frederick R Manby, and Peter J Knowles. Fast linear scaling second-order møller-plesset perturbation theory (mp2) using local and density fitting approximations. *J. Chem. Phys.*, 118(18):8149–8160, 2003.
- [77] Philippe Y Ayala and Gustavo E Scuseria. Linear scaling second-order moller–

- plesset theory in the atomic orbital basis for large molecular systems. *J. Chem. Phys.*, 110(8):3660–3671, 1999.
- [78] M. Schutz, G. Hetzer, and H. J. Werner. Low-order scaling local electron correlation methods. i. linear scaling local mp2. *J. Chem. Phys.*, 111(13):5691–5705, October 1999.
- [79] Bernd Doser, Daniel S Lambrecht, Jörg Kussmann, and Christian Ochsenfeld. Linear-scaling atomic orbital-based second-order møller–plesset perturbation theory by rigorous integral screening criteria. *J. Chem. Phys.*, 130(6):064107, 2009.
- [80] Soohaeng Yoo Willow, Kwang S Kim, and So Hirata. Stochastic evaluation of second-order many-body perturbation energies. *J. Chem. Phys.*, 137(20):204122, 2012.
- [81] Soohaeng Yoo Willow, Matthew R Hermes, Kwang S Kim, and So Hirata. Convergence acceleration of parallel monte carlo second-order many-body perturbation calculations using redundant walkers. *J. Chem. Theory Comput.*, 9(10):4396–4402, 2013.
- [82] Daniel Neuhauser, Eran Rabani, and Roi Baer. Expeditious stochastic approach for mp2 energies in large electronic systems. *J. Chem. Theory Comput.*, 9(1):24–27, 2012.
- [83] Kerstin Andersson, Per-Åke Malmqvist, and Björn O. Roos. Second-order perturbation theory with a complete active space self-consistent field reference function. *J. Chem. Phys.*, 96(2):1218–1226, 1992. doi: <http://dx.doi.org/10.1063/1.462209>. URL <http://scitation.aip.org/content/aip/journal/jcp/96/2/10.1063/1.462209>.

- [84] K. Hirao. Multireference møller-plesset method. *Chem. Phys. Lett.*, 190(3-4): 374–380, 1992. ISSN 0009-2614. doi: [http://dx.doi.org/10.1016/0009-2614\(92\)85354-D](http://dx.doi.org/10.1016/0009-2614(92)85354-D). URL <http://www.sciencedirect.com/science/article/pii/S000926149285354D>.
- [85] Pawel M. Kozlowski and Ernest R. Davidson. Considerations in constructing a multireference second-order perturbation theory. *J. Chem. Phys.*, 100(5):3672–3682, 1994. doi: <http://dx.doi.org/10.1063/1.466355>. URL <http://scitation.aip.org/content/aip/journal/jcp/100/5/10.1063/1.466355>.
- [86] C. Angeli, R. Cimiraglia, S. Evangelisti, T. Leininger, and J.-P. Malrieu. Introduction of  $n$ -electron valence states for multireference perturbation theory. *J. Chem. Phys.*, 114(23):10252–10264, 2001. doi: <http://dx.doi.org/10.1063/1.1361246>. URL <http://scitation.aip.org/content/aip/journal/jcp/114/23/10.1063/1.1361246>.
- [87] Rajat K. Chaudhuri, Karl F. Freed, Gabriel Hose, Piotr Piecuch, Karol Kowalski, Marta Włoch, Sudip Chattopadhyay, Debashis Mukherjee, Zoltán Rolik, Ágnes Szabados, Gábor Tóth, and Péter R. Surján. Comparison of low-order multireference many-body perturbation theories. *J. Chem. Phys.*, 122(13):134105, 2005. doi: <http://dx.doi.org/10.1063/1.1863912>. URL <http://scitation.aip.org/content/aip/journal/jcp/122/13/10.1063/1.1863912>.
- [88] Mark R Hoffmann, Dipayan Datta, Sanghamitra Das, Debashis Mukherjee, Agnes Szabados, Zoltán Rolik, and Péter R Surján. Comparative study of multireference perturbative theories for ground and excited states. *J. Chem. Phys.*, 131(20):204104, 2009.
- [89] Francesco A. Evangelista, Andrew C. Simmonett, Henry F. Schaefer, Debashis

- Mukherjee, and Wesley D. Allen. A companion perturbation theory for state-specific multireference coupled cluster methods. *Phys. Chem. Chem. Phys.*, 11:4728–4741, 2009. doi: 10.1039/B822910D. URL <http://dx.doi.org/10.1039/B822910D>.
- [90] J Paldus, P Piecuch, L Pylypow, and B Jeziorski. Application of hilbert-space coupled-cluster theory to simple  $(h_2)_2$  model systems: Planar models. *Phys. Rev. A*, 47(4):2738–2782, 1993.
- [91] S. Evangelisti, J. P. Daudey, and J. P. Malrieu. Qualitative intruder-state problems in effective hamiltonian theory and their solution through intermediate hamiltonians. *Phys. Rev. A*, 35:4930–4941, Jun 1987. doi: 10.1103/PhysRevA.35.4930. URL <http://link.aps.org/doi/10.1103/PhysRevA.35.4930>.
- [92] Karol Kowalski and Piotr Piecuch. Complete set of solutions of multireference coupled-cluster equations: The state-universal formalism. *Phys. Rev. A*, 61:052506, Apr 2000. doi: 10.1103/PhysRevA.61.052506. URL <http://link.aps.org/doi/10.1103/PhysRevA.61.052506>.
- [93] K. Kowalski and P. Piecuch. Complete set of solutions of the generalized bloch equation. *Int. J. Quantum Chem.*, 80(4-5):757–781, 2000. ISSN 1097-461X. doi: 10.1002/1097-461X(2000)80:4/5<757::AID-QUA25>3.0.CO;2-A. URL [http://dx.doi.org/10.1002/1097-461X\(2000\)80:4/5<757::AID-QUA25>3.0.CO;2-A](http://dx.doi.org/10.1002/1097-461X(2000)80:4/5<757::AID-QUA25>3.0.CO;2-A).
- [94] Björn O. Roos and Kerstin Andersson. Multiconfigurational perturbation theory with level shift – the  $cr_2$  potential revisited. *Chem. Phys. Lett.*, 245(2-3):215–223, 1995. ISSN 0009-2614. doi: [http://dx.doi.org/10.1016/0009-2614\(95\)01010-7](http://dx.doi.org/10.1016/0009-2614(95)01010-7). URL <http://www.sciencedirect.com/science/article/pii/0009261495010107>.

- [95] Cristopher Camacho, Henryk A Witek, and Shigeyoshi Yamamoto. Intruder states in multireference perturbation theory: The ground state of manganese dimer. *J. Comput. Chem.*, 30(3):468–478, February 2009.
- [96] Cristopher Camacho, Renzo Cimiraglia, and Henryk A Witek. Multireference perturbation theory can predict a false ground state. *Phys. Chem. Chem. Phys.*, 12(19):5058–5060, 2010.
- [97] Celestino Angeli, Renzo Cimiraglia, and Jean-Paul Malrieu.  $n$ -electron valence state perturbation theory: A spinless formulation and an efficient implementation of the strongly contracted and of the partially contracted variants. *J. Chem. Phys.*, 117(20):9138–9153, 2002. doi: <http://dx.doi.org/10.1063/1.1515317>. URL <http://scitation.aip.org/content/aip/journal/jcp/117/20/10.1063/1.1515317>.
- [98] Celestino Angeli, Mariachiara Pastore, and Renzo Cimiraglia. New perspectives in multireference perturbation theory: The  $n$ -electron valence state approach. *Theor. Chem. Acc.*, 117(5-6):743–754, 2007. ISSN 1432-881X. doi: 10.1007/s00214-006-0207-0. URL <http://dx.doi.org/10.1007/s00214-006-0207-0>.
- [99] K. G. Dyall. The Choice of a Zeroth-Order Hamiltonian for 2nd-Order Perturbation-Theory with a Complete Active Space Self-Consistent-Field Reference Function. *J Chem. Phys.*, 102(12):4909–4918, 1995.
- [100] Dominika Zgid, Debashree Ghosh, Eric Neuscammann, and Garnet Kin-Lic Chan. A study of cumulant approximations to  $n$ -electron valence multireference perturbation theory. *J. Chem. Phys.*, 130(19):194107, 2009. doi: <http://dx.doi.org/10.1063/1.3132922>. URL <http://scitation.aip.org/content/aip/journal/jcp/130/19/10.1063/1.3132922>.
- [101] Bogumil Jeziorski and Hendrik J. Monkhorst. Coupled-cluster method for

- multideterminantal reference states. *Phys. Rev. A*, 24:1668–1681, Oct 1981. doi: 10.1103/PhysRevA.24.1668. URL <http://link.aps.org/doi/10.1103/PhysRevA.24.1668>.
- [102] U. S. Mahapatra, B. Datta, and D. Mukherjee. A state-specific multi-reference coupled cluster formalism with molecular applications. *Mol. Phys.*, 94(1):157–171, 1998. doi: 10.1080/002689798168448. URL <http://www.tandfonline.com/doi/abs/10.1080/002689798168448>.
- [103] Uttam Sinha Mahapatra, Barnali Datta, and Debashis Mukherjee. A size-consistent state-specific multireference coupled cluster theory: Formal developments and molecular applications. *J. Chem. Phys.*, 110(13):6171–6188, 1999. doi: <http://dx.doi.org/10.1063/1.478523>. URL <http://scitation.aip.org/content/aip/journal/jcp/110/13/10.1063/1.478523>.
- [104] Jiří Pittner, Petr Nachtigall, Petr Čársky, Jozef Mášik, and Ivan Hubač. Assessment of the single-root multireference brillouin-wigner coupled-cluster method: Test calculations on  $\text{ch}_2$ ,  $\text{sih}_2$ , and ttwisted ethylene. *J. Chem. Phys.*, 110(21):10275–10282, 1999. doi: <http://dx.doi.org/10.1063/1.478961>. URL <http://scitation.aip.org/content/aip/journal/jcp/110/21/10.1063/1.478961>.
- [105] Michael Hanrath. An exponential multireference wave-function ansatz. *J. Chem. Phys.*, 123(8):084102, 2005. doi: <http://dx.doi.org/10.1063/1.1953407>. URL <http://scitation.aip.org/content/aip/journal/jcp/123/8/10.1063/1.1953407>.
- [106] Liguo Kong, K R Shamasundar, Ondřej Demel, and Marcel Nooijen. State specific equation of motion coupled cluster method in general active space. *J. Chem. Phys.*, 130(11):114101, 2009.

- [107] Dipayan Datta, Ligu Kong, and Marcel Nooijen. A state-specific partially internally contracted multireference coupled cluster approach. *J. Chem. Phys.*, 134(21):214116, 2011. doi: <http://dx.doi.org/10.1063/1.3592494>. URL <http://scitation.aip.org/content/aip/journal/jcp/134/21/10.1063/1.3592494>.
- [108] Dipayan Datta and Marcel Nooijen. Multireference equation-of-motion coupled cluster theory. *J. Chem. Phys.*, 137(20):204107, 2012.
- [109] Marcel Nooijen, Ondřej Demel, Dipayan Datta, Ligu Kong, K R Shamasundar, V Lotrich, Lee M Huntington, and Frank Neese. Communication: Multireference equation of motion coupled cluster: A transform and diagonalize approach to electronic structure. *J. Chem. Phys.*, 140(8):081102, February 2014.
- [110] Zhenhua Chen and Mark R. Hoffmann. Orbitally invariant internally contracted multireference unitary coupled cluster theory and its perturbative approximation: Theory and test calculations of second order approximation. *J. Chem. Phys.*, 137(1):014108, 2012. doi: <http://dx.doi.org/10.1063/1.4731634>. URL <http://scitation.aip.org/content/aip/journal/jcp/137/1/10.1063/1.4731634>.
- [111] Takeshi Yanai and Garnet Kin-Lic Chan. Canonical transformation theory for multireference problems. *J. Chem. Phys.*, 124(19):194106, 2006. doi: <http://dx.doi.org/10.1063/1.2196410>. URL <http://scitation.aip.org/content/aip/journal/jcp/124/19/10.1063/1.2196410>.
- [112] Takeshi Yanai and Garnet Kin-Lic Chan. Canonical transformation theory from extended normal ordering. *J. Chem. Phys.*, 127(10):104107, 2007. doi: <http://dx.doi.org/10.1063/1.2761870>. URL <http://scitation.aip.org/content/aip/journal/jcp/127/10/10.1063/1.2761870>.

- [113] Eric Neuscamman, Takeshi Yanai, and Garnet Kin-Lic Chan. Strongly contracted canonical transformation theory. *J. Chem. Phys.*, 132(2):024106, 2010.
- [114] Francesco A. Evangelista. A driven similarity renormalization group approach to quantum many-body problems. *J. Chem. Phys.*, 141(5):054109, 2014. doi: <http://dx.doi.org/10.1063/1.4890660>. URL <http://scitation.aip.org/content/aip/journal/jcp/141/5/10.1063/1.4890660>.
- [115] Stefan Kehrein. *The Flow Equation Approach to Many-Particle Systems*. Springer Berlin Heidelberg, 2006.
- [116] Franz Wegner. Flow-equations for hamiltonians. *Annalen der Physik*, 506(2):77–91, 1994. doi: 10.1002/andp.19945060203. URL <http://dx.doi.org/10.1002/andp.19945060203>.
- [117] Koshiroh Tsukiyama, SK Bogner, and A Schwenk. In-medium similarity renormalization group for nuclei. *Phys. Rev. Lett.*, 106(22):222502, 2011.
- [118] K Tsukiyama, SK Bogner, and A Schwenk. In-medium similarity renormalization group for open-shell nuclei. *Phys. Rev. C*, 85(6):061304, 2012.
- [119] H Hergert, SK Bogner, TD Morris, S Binder, A Calci, J Langhammer, and R Roth. Ab initio multireference in-medium similarity renormalization group calculations of even calcium and nickel isotopes. *Phys. Rev. C*, 90(4):041302, 2014.
- [120] ED Jurgenson, Petr Navratil, and RJ Furnstahl. Evolution of nuclear many-body forces with the similarity renormalization group. *Phys. Rev. Lett.*, 103(8):082501, 2009.
- [121] SK Bogner, RJ Furnstahl, and RJ Perry. Similarity renormalization group for nucleon-nucleon interactions. *Phys. Rev. C*, 75(6):061001, 2007.

- [122] Werner Kutzelnigg. Unconventional aspects of coupled-cluster theory. In Petr Čársky, Josef Paldus, and Jirí Pittner, editors, *Recent Progress in Coupled Cluster Methods*, volume 11 of *Challenges and Advances in Computational Chemistry and Physics*, pages 299–356. Springer Netherlands, 2010. ISBN 978-90-481-2884-6. doi: 10.1007/978-90-481-2885-3\_12. URL [http://dx.doi.org/10.1007/978-90-481-2885-3\\_12](http://dx.doi.org/10.1007/978-90-481-2885-3_12).
- [123] Werner Kutzelnigg. How many-body perturbation theory (mbpt) has changed quantum chemistry. *Int. J. Quantum Chem.*, 109(15):3858–3884, 2009. ISSN 1097-461X. doi: 10.1002/qua.22384. URL <http://dx.doi.org/10.1002/qua.22384>.
- [124] Stanisław D. Głazek and Kenneth G. Wilson. Perturbative renormalization group for hamiltonians. *Phys. Rev. D*, 49:4214–4218, Apr 1994. doi: 10.1103/PhysRevD.49.4214. URL <http://link.aps.org/doi/10.1103/PhysRevD.49.4214>.
- [125] Franz Wegner. *Advances in Solid State Physics 40*, chapter Flow equations for Hamiltonians, pages 133–142. Springer Berlin Heidelberg, Berlin, Heidelberg, 2000. ISBN 978-3-540-44560-9. doi: 10.1007/BFb0108350. URL <http://dx.doi.org/10.1007/BFb0108350>.
- [126] Steven R. White. Numerical canonical transformation approach to quantum many-body problems. *J. Chem. Phys.*, 117(16):7472–7482, 2002. doi: <http://dx.doi.org/10.1063/1.1508370>. URL <http://scitation.aip.org/content/aip/journal/jcp/117/16/10.1063/1.1508370>.
- [127] Ingvar Lindgren. A coupled-cluster approach to the many-body perturbation theory for open-shell systems. *Int. J. Quantum Chem.*, 14(S12):33–58, 1978.

ISSN 1097-461X. doi: 10.1002/qua.560140804. URL <http://dx.doi.org/10.1002/qua.560140804>.

- [128] Marcel Nooijen and Rodney J. Bartlett. General spin adaptation of open-shell coupled cluster theory. *J. Chem. Phys.*, 104(7):2652–2668, 1996. doi: <http://dx.doi.org/10.1063/1.471010>. URL <http://scitation.aip.org/content/aip/journal/jcp/104/7/10.1063/1.471010>.
- [129] Björn O Roos, Per Linse, Per EM Siegbahn, and Margareta RA Blomberg. A simple method for the evaluation of the second-order-perturbation energy from external double-excitations with a casscf reference wavefunction. *Chem. Phys.*, 66(1):197–207, 1982.
- [130] Peter Pulay. A perspective on the caspt2 method. *Int. J. Quantum Chem.*, 111(13):3273–3279, 2011. ISSN 1097-461X. doi: 10.1002/qua.23052. URL <http://dx.doi.org/10.1002/qua.23052>.
- [131] Kerstin. Andersson, Per-Åake. Malmqvist, Björn O. Roos, Andrzej J. Sadlej, and Krzysztof Wolinski. Second-order perturbation theory with a casscf reference function. *J. Phys. Chem.*, 94(14):5483–5488, 1990. doi: 10.1021/j100377a012.
- [132] Steven R. White. Density matrix formulation for quantum renormalization groups. *Phys. Rev. Lett.*, 69:2863–2866, Nov 1992. doi: 10.1103/PhysRevLett.69.2863. URL <http://link.aps.org/doi/10.1103/PhysRevLett.69.2863>.
- [133] Garnet Kin-Lic Chan and Martin Head-Gordon. Highly correlated calculations with a polynomial cost algorithm: A study of the density matrix renormalization group. *J. Chem. Phys.*, 116(11):4462–4476, 2002.
- [134] Yuki Kurashige and Takeshi Yanai. Second-order perturbation theory with a density matrix renormalization group self-consistent field reference function:

- Theory and application to the study of chromium dimer. *J. Chem. Phys.*, 135(9):094104, 2011.
- [135] Chenyang Li and Francesco A Evangelista. Multireference Driven Similarity Renormalization Group: A Second-Order Perturbative Analysis. *J. Chem. Theory Comput.*, 11(5):2097–2108, May 2015.
- [136] Werner Kutzelnigg and Debashis Mukherjee. Normal order and extended wick theorem for a multiconfiguration reference wave function. *J. Chem. Phys.*, 107(2):432–449, 1997. doi: <http://dx.doi.org/10.1063/1.474405>. URL <http://scitation.aip.org/content/aip/journal/jcp/107/2/10.1063/1.474405>.
- [137] John A. Pople, J. Stephen Binkley, and Rolf Seeger. Theoretical models incorporating electron correlation. *Int. J. Quantum Chem.*, 10(S10):1–19, 1976. ISSN 1097-461X. doi: [10.1002/qua.560100802](http://dx.doi.org/10.1002/qua.560100802). URL <http://dx.doi.org/10.1002/qua.560100802>.
- [138] J. A. Pople, R. Krishnan, H. B. Schlegel, and J. S. Binkley. Electron correlation theories and their application to the study of simple reaction potential surfaces. *Int. J. Quantum Chem.*, 14(5):545–560, 1978. ISSN 1097-461X. doi: [10.1002/qua.560140503](http://dx.doi.org/10.1002/qua.560140503). URL <http://dx.doi.org/10.1002/qua.560140503>.
- [139] Florian Weigend, Marco Kattannek, and Reinhart Ahlrichs. Approximated electron repulsion integrals: Cholesky decomposition versus resolution of the identity methods. *J. Chem. Phys.*, 130(16):164106, 2009.
- [140] Christof Hättig and Florian Weigend. Cc2 excitation energy calculations on large molecules using the resolution of the identity approximation. *J. Chem. Phys.*, 113(13):5154–5161, 2000.
- [141] Francesco Aquilante, Thomas Bondo Pedersen, Roland Lindh, Björn Olof Roos, Alfredo Sánchez de Merás, and Henrik Koch. Accurate ab ini-

- tio density fitting for multiconfigurational self-consistent field methods. *J. Chem. Phys.*, 129(2):024113, 2008. doi: <http://dx.doi.org/10.1063/1.2953696>. URL <http://scitation.aip.org/content/aip/journal/jcp/129/2/10.1063/1.2953696>.
- [142] Edward G. Hohenstein and C. David Sherrill. Density fitting and cholesky decomposition approximations in symmetry-adapted perturbation theory: Implementation and application to probe the nature of  $\pi$ - $\pi$  interactions in linear acenes. *J. Chem. Phys.*, 132(18):184111, 2010. doi: <http://dx.doi.org/10.1063/1.3426316>. URL <http://scitation.aip.org/content/aip/journal/jcp/132/18/10.1063/1.3426316>.
- [143] A. Eugene DePrince and C. David Sherrill. Accuracy and efficiency of coupled-cluster theory using density fitting/cholesky decomposition, frozen natural orbitals, and a  $t_1$ -transformed hamiltonian. *J. Chem. Theory Comput.*, 9(6):2687–2696, 2013. doi: 10.1021/ct400250u.
- [144] Evgeny Epifanovsky, Dmitry Zuev, Xintian Feng, Kirill Khistyayev, Yihan Shao, and Anna I. Krylov. General implementation of the resolution-of-the-identity and cholesky representations of electron repulsion integrals within coupled-cluster and equation-of-motion methods: Theory and benchmarks. *J. Chem. Phys.*, 139(13):134105, 2013. doi: <http://dx.doi.org/10.1063/1.4820484>. URL <http://scitation.aip.org/content/aip/journal/jcp/139/13/10.1063/1.4820484>.
- [145] Werner Györfy, Toru Shiozaki, Gerald Knizia, and Hans-Joachim Werner. Analytical energy gradients for second-order multireference perturbation theory using density fitting. *J. Chem. Phys.*, 138(10):104104, 2013. doi: <http://dx.doi.org/10.1063/1.4793737>. URL <http://scitation.aip.org/content/aip/journal/jcp/138/10/10.1063/1.4793737>.

- [146] Francesco Aquilante, Per-Åke Malmqvist, Thomas Bondo Pedersen, Abhik Ghosh, and Björn Olof Roos. Cholesky decomposition-based multiconfiguration second-order perturbation theory (cd-caspt2): Application to the spin-state energetics of coiii(diiminato)(nph). *J. Chem. Theory Comput.*, 4(5):694–702, 2008. doi: 10.1021/ct700263h.
- [147] Jonas Boström, Mickaël G. Delcey, Francesco Aquilante, Luis Serrano-Andrés, Thomas Bondo Pedersen, and Roland Lindh. Calibration of cholesky auxiliary basis sets for multiconfigurational perturbation theory calculations of excitation energies. *J. Chem. Theory Comput.*, 6(3):747–754, 2010. doi: 10.1021/ct900612k.
- [148] Frank Neese. The orca program system. *WIREs: Comput. Mol. Sci.*, 2(1): 73–78, 2012. ISSN 1759-0884. doi: 10.1002/wcms.81. URL <http://dx.doi.org/10.1002/wcms.81>.
- [149] Debashis Mukherjee. Normal ordering and a wick-like reduction theorem for fermions with respect to a multi-determinantal reference state. *Chem. Phys. Lett.*, 274(5-6):561–566, 1997.
- [150] Uttam Sinha Mahapatra, Barnali Datta, Barun Bandyopadhyay, and Debashis Mukherjee. State-specific multi-reference coupled cluster formulations: Two paradigms. *Adv. Quantum Chem.*, 30:163–193, 1998. ISSN 0065-3276. doi: [http://dx.doi.org/10.1016/S0065-3276\(08\)60507-9](http://dx.doi.org/10.1016/S0065-3276(08)60507-9). URL <http://www.sciencedirect.com/science/article/pii/S0065327608605079>.
- [151] K. R. Shamasundar. Cumulant decomposition of reduced density matrices, multireference normal ordering, and wicks theorem: A spin-free approach. *J. Chem. Phys.*, 131(17):174109, 2009. doi: <http://dx.doi.org/10.1063/1.>

3256237. URL <http://scitation.aip.org/content/aip/journal/jcp/131/17/10.1063/1.3256237>.
- [152] Liguang Kong, Marcel Nooijen, and Debashis Mukherjee. An algebraic proof of generalized Wick theorem. *J. Chem. Phys.*, 132(23):234107, 2010. doi: <http://dx.doi.org/10.1063/1.3439395>. URL <http://scitation.aip.org/content/aip/journal/jcp/132/23/10.1063/1.3439395>.
- [153] Debalina Sinha, Rahul Maitra, and Debashis Mukherjee. Generalized antisymmetric ordered products, generalized normal ordered products, ordered and ordinary cumulants and their use in many electron correlation problem. *Comput. Theor. Chem.*, 1003:62–70, 2013. ISSN 2210-271X. doi: <http://dx.doi.org/10.1016/j.comptc.2012.09.035>. URL <http://www.sciencedirect.com/science/article/pii/S2210271X12005439>.
- [154] Werner Kutzelnigg and Debashis Mukherjee. Cumulant expansion of the reduced density matrices. *J. Chem. Phys.*, 110(6):2800–2809, 1999.
- [155] David A Mazziotti. Two-electron reduced density matrix as the basic variable in many-electron quantum chemistry and physics. *Chem. Rev.*, 112(1):244–262, 2011.
- [156] Nicholas C. Handy, John A. Pople, Martin Head-Gordon, Krishnan Raghavachari, and Gary W. Trucks. Size-consistent Brueckner theory limited to double substitutions. *Chem. Phys. Lett.*, 164(2-3):185–192, 1989. ISSN 0009-2614. doi: [http://dx.doi.org/10.1016/0009-2614\(89\)85013-4](http://dx.doi.org/10.1016/0009-2614(89)85013-4). URL <http://www.sciencedirect.com/science/article/pii/0009261489850134>.
- [157] I. Shavitt and R. J. Bartlett. *Many-Body Methods in Chemistry and Physics: MBPT and Coupled-Cluster Theory*. Cambridge University Press, Cambridge, UK, 2009.

- [158] H Hergert, SK Bogner, TD Morris, A Schwenk, and K Tsukiyama. The in-medium similarity renormalization group: A novel ab initio method for nuclei. *Phys. Rep.*, 621:165–222, 2016. doi: <http://doi:10.1016/j.physrep.2015.12.007>.
- [159] Florian Weigend, Andreas Köhn, and Christof Hättig. Efficient use of the correlation consistent basis sets in resolution of the identity mp2 calculations. *J. Chem. Phys.*, 116(8):3175–3183, 2002.
- [160] David E. Bernholdt and Robert J. Harrison. Large-scale correlated electronic structure calculations: the ri-mp2 method on parallel computers. *Chem. Phys. Lett.*, 250(5-6):477–484, 1996. ISSN 0009-2614. doi: [http://dx.doi.org/10.1016/0009-2614\(96\)00054-1](http://dx.doi.org/10.1016/0009-2614(96)00054-1). URL <http://www.sciencedirect.com/science/article/pii/0009261496000541>.
- [161] Forte, a suite of quantum chemistry methods for strongly correlated electrons. For the current version, see <https://github.com/evangelistalab/forte>, 2015.
- [162] Justin M. Turney, Andrew C. Simmonett, Robert M. Parrish, Edward G. Hohenstein, Francesco A. Evangelista, Justin T. Fermann, Benjamin J. Mintz, Lori A. Burns, Jeremiah J. Wilke, Micah L. Abrams, Nicholas J. Russ, Matthew L. Leininger, Curtis L. Janssen, Edward T. Seidl, Wesley D. Allen, Henry F. Schaefer, Rollin A. King, Edward F. Valeev, C. David Sherrill, and T. Daniel Crawford. Psi4: An open-source ab initio electronic structure program. *WIREs Comput. Mol. Sci.*, 2(4):556–565, 2012. ISSN 1759-0884. doi: [10.1002/wcms.93](http://dx.doi.org/10.1002/wcms.93). URL <http://dx.doi.org/10.1002/wcms.93>.
- [163] Ambit is a C++ library for the implementation of tensor product calculations through a clean, concise user interface, written by Turney, J. M.; Parrish, R.

- M.; Evangelista, F. A.; Smith, D. G. For the current version, see <https://github.com/jturney/ambit>, 2015.
- [164] Xiangzhu Li and Josef Paldus. Energetics of naphthynes-performance of reduced multi-reference coupled-cluster methods for diradicals 1. *Can. J. Chem.*, 87(7): 917–926, 2009.
- [165] Axel D Becke. Density-functional thermochemistry. iii. the role of exact exchange. *J. Chem. Phys.*, 98(7):5648–5652, 1993.
- [166] Chengteh Lee, Weitao Yang, and Robert G. Parr. Development of the colle-salvetti correlation-energy formula into a functional of the electron density. *Phys. Rev. B*, 37:785–789, 1988. doi: 10.1103/PhysRevB.37.785. URL <http://link.aps.org/doi/10.1103/PhysRevB.37.785>.
- [167] Thom H. Dunning. Gaussian basis sets for use in correlated molecular calculations. i. the atoms boron through neon and hydrogen. *J. Chem. Phys.*, 90(2): 1007–1023, 1989. doi: 10.1063/1.456153. URL <http://link.aip.org/link/?JCP/90/1007/1>.
- [168] M Valiev, E J Bylaska, N Govind, K Kowalski, T P Straatsma, H J J Van Dam, D Wang, J Nieplocha, E Apra, T L Windus, and W A de Jong. Nwchem: A comprehensive and scalable open-source solution for large scale molecular simulations. *Comput. Phys. Commun.*, 181(9):1477–1489, 2010.
- [169] F Albert Cotton. *Chemical Applications of Group Theory*. John Wiley & Sons, 2008.
- [170] David E. Woon and Thom H. Dunning. Gaussian basis sets for use in correlated molecular calculations. iv. calculation of static electrical response properties. *J. Chem. Phys.*, 100(4):2975–2988, 1994. doi: 10.1063/1.466439.

- [171] Florian Weigend. A fully direct ri-hf algorithm: Implementation, optimised auxiliary basis sets, demonstration of accuracy and efficiency. *Phys. Chem. Chem. Phys.*, 4(18):4285–4291, 2002.
- [172] Christof Hättig. Optimization of auxiliary basis sets for ri-mp2 and ri-cc2 calculations: Core-valence and quintuple- $\zeta$  basis sets for h to ar and qzvpp basis sets for li to kr. *Phys. Chem. Chem. Phys.*, 7(1):59–66, 2005.
- [173] Hans Henning Wenk, Michael Winkler, and Wolfram Sander. One century of aryne chemistry. *Angew. Chem. Int. Ed.*, 42(5):502–528, 2003.
- [174] Roberto Sanz. Recent applications of aryne chemistry to organic synthesis. a review. *Org. Prep. Proc. Int.*, 40(3):215–291, 2008.
- [175] Manabu Abe, Jianhuai Ye, and Megumi Mishima. The chemistry of localized singlet 1, 3-diradicals (biradicals): from putative intermediates to persistent species and unusual molecules with a  $\pi$ -single bonded character. *Chem. Soc. Rev.*, 41(10):3808–3820, 2012.
- [176] Roald Hoffmann, Akira Imamura, and Warren J Hehre. Benzynes, dehydroconjugated molecules, and the interaction of orbitals separated by a number of intervening sigma bonds. *J. Am. Chem. Soc.*, 90(6):1499–1509, 1968.
- [177] Robert R Squires and Christopher J Cramer. Electronic interactions in aryne biradicals. ab initio calculations of the structures, thermochemical properties, and singlet-triplet splittings of the didehydronaphthalenes. *J. Phys. Chem. A*, 102(45):9072–9081, 1998.
- [178] Paul G Wenthold, Robert R Squires, and WC Lineberger. Ultraviolet photoelectron spectroscopy of the o-, m-, and p-benzyne negative ions. electron affinities and singlet-triplet splittings for o-, m-, and p-benzyne. *J. Am. Chem. Soc.*, 120(21):5279–5290, 1998.

- [179] Christopher J Cramer. Bergman, aza-Bergman, and protonated aza-Bergman cyclizations and intermediate 2,5-arynes: Chemistry and challenge to computation. *J. Am. Chem. Soc.*, 120(25):6261–6269, 1998.
- [180] T Daniel Crawford, E Kraka, John F Stanton, and Dieter Cremer. Problematic *p*-benzyne: Orbital instabilities, biradical character, and broken symmetry. *J. Chem. Phys.*, 114(24):10638–10650, 2001.
- [181] Francesco A Evangelista, Wesley D Allen, and Henry F Schaefer III. Coupling term derivation and general implementation of state-specific multireference coupled cluster theories. *J. Chem. Phys.*, 127(2):024102, 2007.
- [182] Evan B Wang, Carol A Parish, and Hans Lischka. An extended multireference study of the electronic states of *para*-benzyne. *J. Chem. Phys.*, 129(4):044306, 2008.
- [183] Jiří Brabec, Sriram Krishnamoorthy, Hubertus JJ van Dam, Karol Kowalski, and Jiří Pittner. Massively parallel implementation of the multireference brillouin–wigner ccSD method. *Chem. Phys. Lett.*, 514(4):347–351, 2011.
- [184] Jiří Brabec, Kiran Bhaskaran-Nair, Karol Kowalski, Jiří Pittner, and Hubertus JJ van Dam. Towards large-scale calculations with state-specific multireference coupled cluster methods: Studies on dodecane, naphthynes, and polycarbenes. *Chem. Phys. Lett.*, 542:128–133, 2012.
- [185] Ivan Hubač, Jiří Pittner, and Petr Čársky. Size-extensivity correction for the state-specific multireference brillouin–wigner coupled-cluster theory. *J. Chem. Phys.*, 112(20):8779–8784, 2000.
- [186] Nicholas J Mayhall and Martin Head-Gordon. Increasing spin-flips and decreasing cost: Perturbative corrections for external singles to the complete active

- space spin flip model for low-lying excited states and strong correlation. *J. Chem. Phys.*, 141(4):044112, July 2014.
- [187] Florian Weigend and Reinhart Ahlrichs. Balanced basis sets of split valence, triple zeta valence and quadruple zeta valence quality for h to rn: Design and assessment of accuracy. *Phys. Chem. Chem. Phys.*, 7(18):3297–3305, 2005.
- [188] Jan Almlöf. Elimination of energy denominators in Møller–Plesset perturbation theory by a Laplace transform approach. *Chem. Phys. Lett.*, 181(4):319–320, 1991.
- [189] Marco Häser and Jan Almlöf. Laplace transform techniques in Møller–Plesset perturbation theory. *J. Chem. Phys.*, 96(1):489, 1992.
- [190] Daniel S Lambrecht, Bernd Doser, and Christian Ochsenfeld. Rigorous integral screening for electron correlation methods. *J. Chem. Phys.*, 123(18):184102, 2005.